PESARO 2017

The Seventh International Conference on Performance, Safety and Robustness in Complex Systems and Applications

ISBN: 978-1-61208-549-4

April 23 - 27, 2017

Venice, Italy

PESARO 2017 Editors

Wolfgang Leister, Norsk Regnesentral (Norwegian Computing Center), Norway
Mohammad Rajabali Nejad, University of Twente, the Netherlands
Michael Hübner, Ruhr-University Bochum, Germany

PESARO 2017

Forward

The Seventh International Conference on Performance, Safety and Robustness in Complex Systems and Applications (PESARO 2017), held between April 23-27, 2017 in Venice, Italy, continued a series of special events dedicated to fundamentals, techniques and experiments to specify, design, and deploy systems and applications under given constraints on performance, safety and robustness.

There is a relation between organizational, design and operational complexity of organization and systems and the degree of robustness and safety under given performance metrics. More complex systems and applications might not be necessarily more profitable, but are less robust. There are trade-offs involved in designing and deploying distributed systems. Some designing technologies have a positive influence on safety and robustness, even operational performance is not optimized. Under constantly changing system infrastructure and user behaviors and needs, there is a challenge in designing complex systems and applications with a required level of performance, safety and robustness

The conference had the following tracks:

- Safety
- ESITIS: Evolution of Safety in Transportation and Industrial Systems
- MAIS: Machine Learning Algorithms in Image and Signal Processing

We take here the opportunity to warmly thank all the members of the PESARO 2017 technical program committee, as well as all the reviewers. The creation of such a high quality conference program would not have been possible without their involvement. We also kindly thank all the authors that dedicated much of their time and effort to contribute to PESARO 2017. We truly believe that, thanks to all these efforts, the final conference program consisted of top quality contributions.

We also gratefully thank the members of the PESARO 2017 organizing committee for their help in handling the logistics and for their work that made this professional meeting a success.

We hope that PESARO 2017 was a successful international forum for the exchange of ideas and results between academia and industry and to promote further progress in the area of performance, safety and robustness in complex system. We also hope that Venice, Italy provided a pleasant environment during the conference and everyone saved some time to enjoy the unique charm of the city.

PESARO 2017 Committee

PESARO Steering Committee

Wolfgang Leister, Norsk Regnesentral (Norwegian Computing Center), Norway
Mohammad Rajabali Nejad, University of Twente, the Netherlands

Omar Smadi, Iowa State University, USA
Yulei Wu, University of Exeter, UK

PESARO Industry/Research Advisory Committee
John Favaro, INTECS, Italy
Jean-Pierre Seifert, TU Berlin & FhG SIT Darmstadt, Germany
Roger Rivett, Jaguar Land Rover, UK

PESARO 2017
Committee

PESARO Steering Committee

Wolfgang Leister, Norsk Regnesentral (Norwegian Computing Center), Norway
Mohammad Rajabali Nejad, University of Twente, the Netherlands
Omar Smadi, Iowa State University, USA
Yulei Wu, University of Exeter, UK

PESARO Industry/Research Advisory Committee

John Favaro, INTECS, Italy
Jean-Pierre Seifert, TU Berlin & FhG SIT Darmstadt, Germany
Roger Rivett, Jaguar Land Rover, UK

PESARO 2017 Technical Program Committee

Morteza Biglari-Abhari, University of Auckland, New Zealand
Andrea Ceccarelli, University of Florence, Italy
Salimur Choudhury, Algoma University, Canada
Dieter Claeys, Ghent University, Belgium
Frank Coolen, Durham University, UK
Faten Fakhfakh, University of Sfax, Tunisia
John Favaro, INTECS, Italy
Francesco Flammini, Ansaldo STS – Innovation, Italy
Víctor Flores Fonseca, Universidad Católica del Norte, Chile
John-Austen Francisco, Rutgers, the State University of New Jersey, USA
Denis Gingras, Université de Sherbrooke, Canada
Teresa Gomes, University of Coimbra, Portugal
Denis Hatebur, University Duisburg-Essen, Germany
Mohamed Hibti, EDF R&D, France
C. Michael Holloway, Safety-Critical Avionics Systems Branch | NASA Langley Research Center, Hampton, Virginia, USA
Rémy Houssin, University of Strasbourg, France
Michael Hübner, Ruhr-University of Bochum, Germany
Christos Kalloniatis, University of the Aegean, Greece
Atsushi Kanai, Hosei University, Japan
Sokratis K. Katsikas, Norwegian University of Science & Technology (NTNU), Norway
M.-Tahar Kechadi, University College Dublin (UCD), Ireland
Peter Kieseberg, SBA Research, Austria
Anastasios Kouvelas, École Polytechnique Fédérale de Lausanne, Switzerland

Thorsten Kramp, IBM Research Zurich, Switzerland
Wolfgang Leister, Norsk Regnesentral (Norwegian Computing Center), Norway
Olaf Maennel, Tallinn University of Technology, Estonia
Stefano Marrone, Seconda Università di Napoli, Italy
Markos Papageorgiou, Technical University Of Crete, Greece
Mohammad Rajabali Nejad, University of Twente, Netherlands
Mohsen Ramezani, University of Sydney, Australia
Roger Rivett, Jaguar Land Rover, UK
Jean-Pierre Seifert, TU Berlin & FhG SIT Darmstadt, Germany
Luis Enrique Sánchez Crespo, University of Castilla-La Mancha, Spain
Omar Smadi, Iowa State University, USA
Elias Stipidis, Vetronics Research Centre (VRC) | University of Brighton, UK
Young-Joo Suh, POSTECH (Pohang University of Science and Technology), Korea
M'hamed Tahiri, Ecole Nationale Supérieure des Mines de Rabat (ENSMR), Morocco
Hironori Washizaki, Waseda University, Japan
Safwan Wshah, PARC - a Xerox company, Webster, USA
Yulei Wu, University of Exeter, UK
Piotr Zwierzykowski, Poznan University of Technology, Poland

Copyright Information

For your reference, this is the text governing the copyright release for material published by IARIA.

The copyright release is a transfer of publication rights, which allows IARIA and its partners to drive the dissemination of the published material. This allows IARIA to give articles increased visibility via distribution, inclusion in libraries, and arrangements for submission to indexes.

I, the undersigned, declare that the article is original, and that I represent the authors of this article in the copyright release matters. If this work has been done as work-for-hire, I have obtained all necessary clearances to execute a copyright release. I hereby irrevocably transfer exclusive copyright for this material to IARIA. I give IARIA permission or reproduce the work in any media format such as, but not limited to, print, digital, or electronic. I give IARIA permission to distribute the materials without restriction to any institutions or individuals. I give IARIA permission to submit the work for inclusion in article repositories as IARIA sees fit.

I, the undersigned, declare that to the best of my knowledge, the article is does not contain libelous or otherwise unlawful contents or invading the right of privacy or infringing on a proprietary right.

Following the copyright release, any circulated version of the article must bear the copyright notice and any header and footer information that IARIA applies to the published article.

IARIA grants royalty-free permission to the authors to disseminate the work, under the above provisions, for any academic, commercial, or industrial use. IARIA grants royalty-free permission to any individuals or institutions to make the article available electronically, online, or in print.

IARIA acknowledges that rights to any algorithm, process, procedure, apparatus, or articles of manufacture remain with the authors and their employers.

I, the undersigned, understand that IARIA will not be liable, in contract, tort (including, without limitation, negligence), pre-contract or other representations (other than fraudulent misrepresentations) or otherwise in connection with the publication of my work.

Exception to the above is made for work-for-hire performed while employed by the government. In that case, copyright to the material remains with the said government. The rightful owners (authors and government entity) grant unlimited and unrestricted permission to IARIA, IARIA's contractors, and IARIA's partners to further distribute the work.

Table of Contents

Fall Detection of the Elderly in the Activities of Daily Living 1
Taekyeong Lee, Youngho Lee, Jaemin Kim, Soonmoon Jung, Dongwook Yang, Beomgeun Jo, Jeongwoo Lee, and Junghwa Hong

Determination of the Environmental Conditions by the Evaluation of Test Drive Data 3
Steffen Wittel, Daniel Ulmer, and Oliver Buhler

Measuring Safety in Aviation: Empirical Results about the Relation between Safety Outcomes and Safety Management System Processes, Operational Activities and Demographic Data 9
Steffen Kaspers, Nektarios Karanikas, Alfred Roelen, Selma Piric, Robbert van Aalst, and Robert Jan de Boer

ERTMS Challenges for a Safe and Interoperable European Railway System 17
Katja Schuitemaker and Mohammad Rajabalinejad

Supporting Risk-Based Design by Computational Synthesis 23
Mohammad Rajabalinejad, Robert Velten, and Hans Tragter

Shift-Invariant Motif Discovery in Image Processing 27
Sahar Torkamani and Volker Lohweg

A Survey on CNN and RNN Implementations 33
Javier Hoffmann, Osvaldo Navarro Guzman, Florian Kastner, Benedikt Janssen, and Michael Hubner

Fall Detection of the Elderly in the Activities of Daily Living

Taekyeong Lee, Youngho Lee, Jaemin Kim, Soonmoon Jung, Dongwook Yang, Beomgeun Jo, Jeongwoo Lee and Junghwa Hong*
Dept. of Control and Instrumentation Engineering
Korea University
Sejong, South Korea
E-mail: kenya9802, astrots, jaemini, moonol3, tellmeting, bumga91, jeong8523, *hongjh32@korea.ac.kr

***Abstract*—Falling of the elderly has become an important issue in today's aging society. As a result, active protecting devices are being developed to protect the fallers' body from severe injuries. The key task of the protecting devices is the exact detection of a falling event in Activities of Daily Living (ADL). In this study, a methodology for detecting the fall event is proposed using the accelerometer and the gyro-sensor of an active protecting device. The results of fall detection using the methodology proposed in this study were detected before impact and are accurate more than 99.9 % for ADL.**

Keywords-fall detection; double threshold algorithm; ADL; fall injury; Savitzky-Golay filter.

I. INTRODUCTION

More than 30% of the elderly over the age of 65 years have experienced at least one fall per year [1]-[2], which significantly deteriorates quality of life. Furthermore, approximately 15,800 adults over 65 years of age died from injuries related to unintentional falls in the USA. Also, about 1.8 million people over 65 years of age who had non-fatal injuries visited the emergency departments and spent $19 billion in the year 2000 in the USA [3]. Falls of the elderly while doing different activities occur in the bath room (26%), in the living room or bed room (26%), on the stairs (10%), in the hall way (8%), and outside of the house (20%) [4]. Based on movements, the elderly fall during level walking (43 %), going in-and-out of a bathroom (30%), sitting down and standing up from a seating position (13%), and in ascending and descending stairs (15%) [4]. The postural imbalance in activities and movements is caused by tripping or slipping (27.4%); surrounding hazards, for example, wet or uneven floor (21.8%); misjudging, overbalancing, or over-reaching (17.8%); and fainting, dizziness, illness, or legs giving way (17.7%) [5], which are part of the Activities of Daily Living (ADL). Many of these falls may be avoided if fall risk assessment and prevention tools where available as an integral part of ADL. However, the fall risk assessment is still not completed at this moment. Currently, active protecting devices for people falling are being developed to protect the person's body from severe injuries as an alternative or for a practical purpose. For these developments, the exact detection of the fall is important for active control of the protecting devices. Since the falls involve very complex body movements, a precise detection of the fall events is a very challenging task, particularly for industrial applications. In this study, a methodology for detecting the fall events is proposed using an accelerometer and a gyro-sensor for an active protecting device from the fall injuries.

The rest of the paper is structured as follows. In Section 2, the fall experimental method in ADL to obtain data and the fall detection algorithm are explained. In Section 3, the results of fall detection using proposed algorithm are explained and a conclusion is given.

II. MATERIALS AND METHODS

A. The fall experiments in ADL

21 male subjects participated in the experiment to obtain fall data. The 3D accelerometer (LIS3DSH, ± 16 g, 0.73 mg/digit), gyro-sensor (L3G4200D, ± 2000 Deg/sec, 70 mdps/digit), and compass (HMC5883L, ± 8 Gauss, 5 milli-gauss) were put on the sacrum of the subjects for the fall experiments during level walking, sitting down, ascending and descending stairs. In addition, the 3D kinematics of the lower limbs and upper body during the locomotion or movements were measured using a stereo photogrammetric system, which consisted of seven infrared emitting Charge Coupled Device (CCD) cameras (Motion Analysis System, USA). The data from the sensors was transmitted in a wireless manner using Radio Frequency (RF) (nRF2401+, 2.4GHz). Fig. 1 shows the experimental setups and an example of the fall experiments. A slider was used to induce a fall perturbation.

B. The fall detection algorithm

In order to be applied to active protecting devices, fall detection must be precisely performed just after the start of the fall event, which is, when the falling person cannot return to the balanced posture. For fall detection, the accelerations, angular velocities, and angle at the sacrum, thus pelvis, were used. Based on the resulting acceleration (see Figure 2) a fall event could be classified as Fall 1- the period from the start of the fall to the lowest peak, and Fall 2- the period from the lowest peak to the impact. For perfect protection of the falling persons' body, the detection should be accomplished within Fall 1. At the same time, the detection must be capable of discerning real fall from movements in ADL. In

Copyright (c) IARIA, 2017. ISBN: 978-1-61208-549-4

this study, the experimental data collected from ADL, such as the level, slope, and stair gait, as well as the sit down and up motions, were statistically analyzed to obtain the fall criteria. The fall criteria were determined based on the superior-inferior and resultant accelerations, pelvic tilt and obliquity angles, and resultant angular velocity. The signals from the sensors were processed for the reduction of moving artifacts and random noises using the Savitzky-Golay filter [6]. Then, the onset of the fall using the criteria was detected after applying the double threshold algorithm [7].

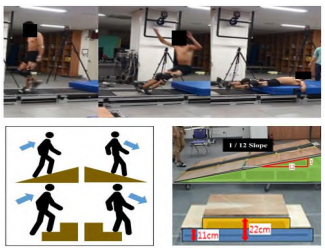

Figure 1. The fall test and experimental equipment

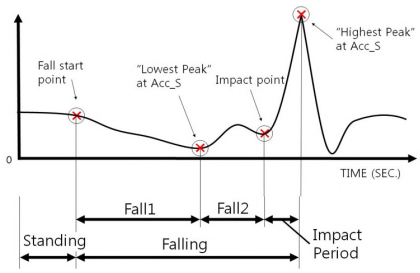

Figure 2. The fall event based on the resultant acceleration

III. RESULTS AND CONCLUSION

After analyzing the data collected from movements in ADL, the summation of acceleration at the sacrum could detect almost all movements of the fall, such as for level walking, stairs, slope, sit up and down, except the falls happening during running. The pelvic tilt, superior-inferior acceleration, and resultant angular velocity could discern real falls from all movements in ADL, except in sit up and down, and lay down cases.

Fig. 3 shows the flow for detecting a fall. In the case of level walking, the fall onset time after applying the perturbation by the slider was faster than the lowest peak point by as much as 0.105 sec. In addition, the fall onset time by the bump trap was earlier than the lowest peak point by as much as 0.329 sec. In general, the fall onsets by applying all perturbations were detected before the lowest peak points for all movements in ADL situations. Table 1 shows threshold ranges and detecting capabilities of the fall criteria. STS means motions in the sit down and up. The detections were accurate more than 99.9 % for 5 categories in ADL, as indicated in Table 1, based on the field experiments, which were performed for the elderly in a retirement home. Further research is required for the detecting capabilities in case of non-ADL situations.

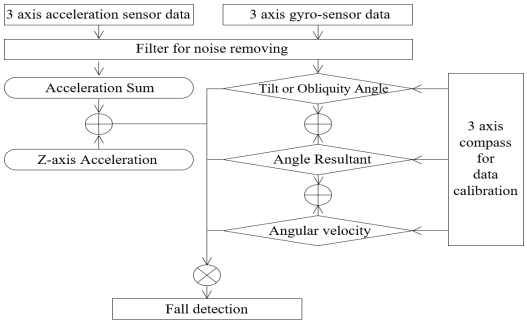

Figure 3. The fall detection algorithm flow chart

TABLE 1. THRESHOLD RANGE ANALYSIS RESULTS IN ADL

	ADL (Activities of daily living)							Threshold range
	Walking	Running	Slope	Stair	Stumble	STS	Lie down	
Acc_Z	○	X	○	○	○	X	X	0.23~0.35 g
Acc_Sum	○	X	○	○	○	○	○	0.36~0.4 g
AngV_R	○	○	○	○	○	X	X	105~135 Deg/sec
Tilt	○	○	○	○	○	X	X	26~58 Deg
Obliquity	○	○	○	○	○	○	○	21~43 Deg
Angle_R	○	○	○	○	○	X	X	30~46 Deg

○: Distinct motion from fall by IMU sensor
X: Not distinct motion from fall by IMU sensor

ACKNOWLEDGMENT

This work was supported by the Industrial Strategic Technology Development Program (No.10048732) funded by the Korean Ministry of Trade, industry & Energy, and the Korea Health Technology R&D Project (HI15C1025) funded by the Korean Ministry of Health & Welfare.

REFERENCES

[1] S. D. Berry and R. R. Miller, "Falls: epidemiology, pathophysiology, and relationship to fracture," Current osteoporosis reports, 2008, vol. 6, pp. 149-154.

[2] S. W. Muir, K. Berg, B. Chesworth, N. Klar, and M. Speechley, "Balance impairment as a risk factor for falls in community-dwelling older adults who are high functioning: a prospective study," Physical therapy, 2010, vol. 90, pp. 338-347.

[3] A. J. Sai, J. C. Gallagher, L. M. Smith, and S. Logsdon, "Fall predictors in the community dwelling elderly: a cross sectional and prospective cohort study," J Musculoskelet Neuronal Interact, 2010, vol. 10, pp. 142-150.

[4] W. L. Watson and R. Mitchell, "Conflicting trends in fall-related injury hospitalisations among older people: variations by injury type," Osteoporosis Int, 2011, vol. 22, pp. 2623-2631.

[5] A. J. Milat et al, "Prevalence, circumstances and consequences of falls among community-dwelling older people: results of the 2009 NSW falls prevention baseline survey," New South Wales public health bulletin, vol. 22, pp. 43-48, 2011.

[6] J. Luo, K. Ying, and J. Bai, "Savitzky-Golay smoothing and differentiation filter for even number data," Signal Processing, 2005, vol. 85, pp. 1429-1434.

[7] J. Vartiainen, J. J. Lehtomaki, and H. Saarnisaari, "Double-threshold based narrowband signal extraction," In Vehicular Technology Conference 2005. VTC 2005-Spring. 2005 IEEE 61st, IEEE, Jan. 2005, Vol.2, pp. 1288-1292.

Determination of the Environmental Conditions by the Evaluation of Test Drive Data

Steffen Wittel*, Daniel Ulmer* and Oliver Bühler*
*Steinbeis Interagierende Systeme GmbH, Esslingen, Germany
Email: {steffen.wittel,daniel.ulmer,oliver.buehler}@interagierende-systeme.de

***Abstract*—With taking full responsibility for the driving maneuvers automatically performed by the vehicles, the automobile manufacturers are responsible that the vehicles can handle the spectrum of possible traffic situations in the automated driving mode. The vehicles have to either cope with the traffic situations without the help of the human driver or to handover the control to the human driver in a safe manner. For the handover, a reasonable warning period is required, in which the automated driving has to be maintained. Therefore, the warning period depends on the distraction of the human driver and the current traffic situation. The time must be sufficient, so that the human driver can perceive the traffic situation and react appropriately. The testing of automated driving is considered as a major challenge for the automotive industry, because so far the human driver was considered as an immediate fallback level in traffic situations that cannot be handled by the vehicle software. Hence, robustness testing becomes more and more important to ensure a safe operation of the vehicles within different environmental conditions. This paper presents an approach that determines the environmental conditions encountered during test drives based on traffic theory. The approach provides metrics, which describe the traffic situations of test drives from an environmental point of view. Hence, the consideration of the metrics can ensure comparable traffic situations for the evaluation of the vehicle behavior between different versions of an automated driving system. Moreover, they can point to areas of the vehicle software that have not yet been tested and thus can be used to track the progress of the testing during the development.**

Keywords–Automated Driving; Environmental Conditions; Test Drives.

I. Introduction

Driving in a dynamic environment is subject to a variety of cognitive demands of the human driver as shown in [2]. The human driver has to correctly perceive the traffic situation, interpret it, and derive actions from it. Moreover, she or he has to recognize new circumstances and make appropriate adjustments well enough in advance. Overall, driving is a complex task and offers the possibility to make mistakes. Approximately 94 % of the road accidents, as published in [3], are caused by the human driver due to incorrect performing of driving maneuvers, wrong decisions or carelessness. Therefore, the human driver is considered as the main cause of the majority of all road accidents, which offers a great potential to improve the traffic safety by the automation of driving. The automated driving relieves thereby the human driver of specific driving tasks in certain driving scenarios.

The road accidents statistic [1] based on the police reporting in Germany covers mainly road accidents with serious consequences and usually none with material damages or minor injuries. For each reported road accident, the police determine the main cause that led to the road accident, which is part of the statistic. The main causes provided by the Federal Statistical Office of Germany [4], as summarized in Figure 1, shows that a large number of road accidents in urban environments (about 40 %) could not be assigned to one of the major causes listed in the summary. Collisions at intersections (32.8 %) are the main cause for road accidents in urban environments, whereas leaving the carriageway (32.3 %) is the main cause in non-urban environments. The main cause of almost half of all road accidents on the freeways that represent only a small percent of the entire road network of Germany, but with a high dwell time of the road users, are rear-end collisions followed by leaving the carriageway (27.5 %) and collisions during the lane change (13.5 %). Almost 90 % of all road accidents on the freeways can be assigned to three causes, which can be extensively tested by the automobile manufacturers. Hence, it is hardly surprising that they are going to provide their first automated driving functions for the use on freeways [5]. Freeways provide a manageable complexity, both in the tasks to be performed by the driver of a vehicle and in their construction. Simplified, it can be said that the vehicle control is limited to approaching and overtaking other vehicles. The characteristics of a freeway are usually clearly defined by the government, e.g., in the German Road Traffic Act as shown below:

a) Only for motor vehicles
b) Entry and exit only at marked locations
c) Traffic on the continuous road has the right of way
d) Turning and reversing are prohibited
e) Stopping is prohibited

According to SAE J3016 [6], the currently available comfort functions for specific driving scenarios, i.e., an Adaptive Cruise Control or a Parking Assist, belong to the driving automation level ”Partial Automation”. In this driving automation level, the vehicle control is automated in the lateral and in longitudinal direction. Thereby, the human driver is considered as an immediate fallback level in traffic situations, which cannot be handled by the vehicle. The next generation of comfort functions will belong to the next higher driving automation level ”Conditional Automation”. After a warning of the system, the human driver has to react only within a reasonable time. The necessary time for the handover of the vehicle control, which is expected to be in the double-digit seconds range [7], differs depending on the degree of distraction of the human driver and the complexity of the current traffic situation. This means, e.g., that a handover just before a collision, in which the human driver has no possibility to avoid the collision, is not acceptable.

The spectrum of possible traffic situations and their temporal sequences in the road traffic are challenges for the automated driving. In practice, they are usually not adequately considered by current test methods and thus it is hardly possible to draw any conclusions about the robustness of the vehicle

Copyright (c) IARIA, 2017. ISBN: 978-1-61208-549-4

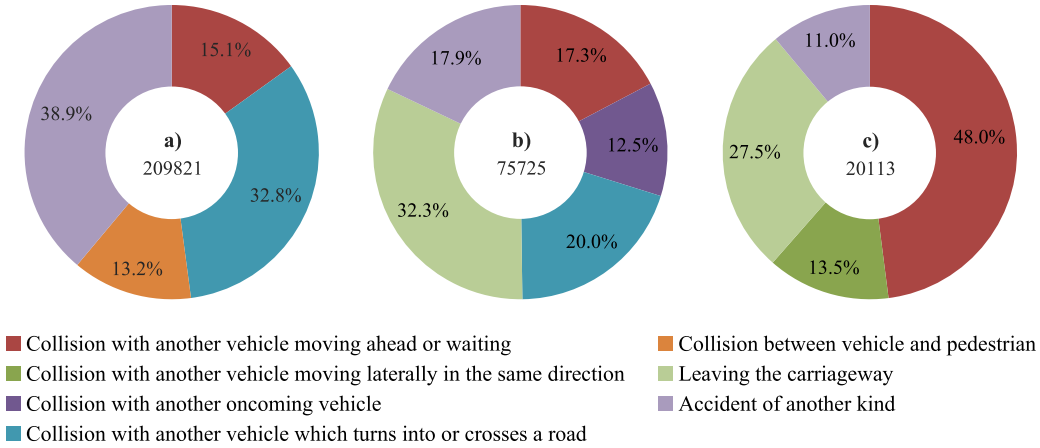

Figure 1. Summary about road accidents in Germany in 2015 [1] separated by the street location: a) urban environments b) non-urban environments c) freeways.

software. In contrast to a drive within a defined environment, an automated vehicle has to cope with a large number of different environmental conditions in the road traffic. Therefore, not only the starting point and the destination are critical factors of a drive, but also a combination of many factors unknown before. Drives between the same starting point and destination differ at least in the number of encountered road users and their driving behavior. In any case, the automobile manufacturers have to ensure that the vehicle reaches its intended destination or a safe state without endangering the occupants or other road users in compliance with the road traffic regulations.

The following section shows the related work. In Section III, an approach is presented, which determines the environmental conditions encountered during test drives based on traffic theory to provide metrics, which describe the traffic situations of the test drives from an environmental point of view. The metrics represent, among others, the complexity and the criticality of the coped traffic situations. Based on these metrics, the vehicle behavior can be evaluated in similar traffic situations to find deviations from the specification. The metrics can also point to areas of the vehicle software that have not yet been tested and thus they can be used to track the progress of the testing during the development. Finally, Section IV shows a case study to discuss the idea behind the presented approach on the example of a simulated drive on the freeway.

II. Related Work

In [8], the authors claim that in relation to automated driving the definitions of the terms ”scene”, ”situation” and ”scenario” are often vague or even contradictory. To cope with this, they did a review of existing definitions including a detailed comparison between them. Moreover, the authors suggest their own definition and provide an example, which demonstrates the usage of the definition, for each term. According to these definitions, a scene describes a snapshot of the environment that is all-encompassing only in the simulation, whereas it is incomplete, incorrect, uncertain and subjective in the real world. A situation can be derived from a scene, which is defined as the entirety of circumstances and entails all relevant conditions, options and determinants. A sequence of scenes forms a scenario that describes the temporal development.

The study [9] shows that there is currently a lack of metrics, which can be used to compare different versions of an automated driving system. In [10], it is assumed that a single metric has no significance and that comparability can only be achieved by using several independent metrics. Moreover, it is shown that reaching a statistical goal does not make a statement about the coped traffic situations during the test drives and therefore cannot be used as an appropriate metric. The authors argue that no real test drive is identical, even if it is performed between the same starting point and destination. Thus, test methods using systematic approaches, taking into account the time behavior, are required, which cover a wide spectrum of the system input and have a better performance than brute force. According to [11], simulation can offer a way to perform the expected number of tests.

Different data collection methods are explained in [12], which can be used to monitor the road traffic. Thereby the authors differ between trajectory data, floating-car data and cross-sectional data. The trajectory data is determined by recording the position of all vehicles within a defined area from one or more external observation points for a certain time. It allows the direct determination of the road traffic density and the lane changes. Floating-car data are captured from specially equipped vehicles, which are part of the road traffic. They record their location obtained from the GPS and their speed. In contrast to floating-car data, cross-sectional data are captured by detectors.

An approach is described in [13] that evaluates the criticality of traffic scenarios from the viewpoint of an external observer by using a parameterizable distance model. The model spans safety areas around the road users, which are dynamically adapted to the current traffic situation. Thereby, the dynamic behavior of the distance model allows, e.g., an increase in the size of the safety areas in specific directions depending on the velocity of the road users. The authors argue that the safe distance between road users depends on the traffic situation and cannot be specified by generally valid values. These values, which are considered as safe, vary, among others, with the driving direction or the environmental conditions. In the presented case study, the distance model was parameterized according to the two-second rule, which states that a driver of

a vehicle should stay at least two seconds behind the vehicle in front. Based on the information provided by the distance model, a classification of the current traffic situation was done using the three classes: ”unsuspicious”, ”hazardous” or ”event of damage”.

III. Approach for Test Drives

During the development, different versions of an automated driving system have to be evaluated to decide whether the changes made have only the desired and no unintended effects. Especially with real vehicles, it is difficult to reproduce the environmental conditions and the temporal development as specified in the test scenarios, and thus to decide if a test scenario was executed as specified and if the evaluation criteria are passed or not. Only if the test scenario was executed as specified, the behavior of the vehicle can be compared between different test runs. As discussed in [9], there is currently a lack of metrics, on the basis of which a decision can be made. The presented approach shall close this gap by providing metrics about the traffic situations of test drives that represent the encountered environmental conditions and the behavior of the test vehicle. With the help of such metrics, the approach allows the developers and testers not only to compare the data, but also to have a better understanding of the vehicle behavior within different environmental conditions. Moreover, the metrics can be used to track the progress of the testing by showing areas that have not yet been tested or areas that have an above-average coverage rate. An above-average test coverage rate does not necessarily increase the quality of the automated driving system, but rather reduces the efficiency of the testing.

The presented approach not only works with data from simulations, but also with data captured from real test vehicles. Within an all-knowing simulation, the entire data of the test drive are available, whereas the data from a real test vehicle only contains the information within the sensor range of the vehicle. The information outside of the sensor range is therefore considered as not relevant for the approach.

A. Evaluation of the Test Drive Data

The test vehicle and the other road users, also called objects, are both part of the road traffic and therefore they can influence each other. The trajectory data of the road users describe their dynamic behavior and possible influences on a high abstraction level from the viewpoint of an outside observer. In addition, information about the road characteristics is required to determine the orientation of the test vehicle on the road. Some information depends on the vehicle line. Other information is obtained from sensors of the test vehicle that provide physical quantities about the test vehicle itself and its environment. The road characteristics are obtained from vehicle-mounted cameras or high-definition maps. All the required information and data are stored within an internal representation of the test drive. Overall, the following information is evaluated by the approach:

a) Test vehicle
   1) Length and width
   2) Mounting positions of the sensors
   3) Absolute velocity
   4) Absolute acceleration

b) Environment
   1) Object sizes
   2) Relative object positions
   3) Relative object velocities
   4) Relative object accelerations
   5) Lane types
   6) Lane positions

B. Determination of the Environmental Conditions

Based on the internal representation, a determination of the environmental conditions is performed by the approach. Therefore, it is sufficient to analyze only the information within the sensor range of the test vehicle as described before. Objects outside of the sensor range have no direct influence on the current behavior of the automated driving system and only play a role, when they are coming into the sensor range at a later point in time or have an influence on objects within the sensor range. The approach provides the following data about the environmental conditions:

a) Velocity of the road users
b) Acceleration of the road users
c) Jerk of the road users (third derivative of the displacement)
d) Distance between two road users
e) Time to the preceding road user
f) Time to the following road user
g) Collisions between road users
h) Traffic density (number of road users within a road segment at a point in time)
i) Traffic flow (number of road users that cross a point on the road within a period of time)

If necessary, the road users are expanded around the center of gravity and thus collisions with other road users are checked. In case of a road with several lanes, a separate analysis is performed for each lane.

For a first overview of the traffic situations, the spatio-temporal context, which reflects the place and the time, is used to characterize the type and the properties of motion [14] as commonly applied in the traffic theory. In this way, aggregated values (e.g., for the density, the velocity and the acceleration) are provided for defined road sections at certain periods of time. This is followed by a detailed analysis of the dynamic behavior of the test vehicle, which can be experienced directly by its passengers. Therefore, the approach analyzes the third derivative of the displacement, named jerk, to find points in time with rapid changes in the dynamics that exceed a limit.

Metrics are provided by the approach for the complexity and the criticality of a traffic situation, and how the test vehicle handles the traffic situation. The complexity metric is determined on the basis of the road characteristics, as well as on the traffic density and the traffic flow in the surroundings of the test vehicle. The criticality metric is calculated based on the evaluation of the distances to other road users and their changes, as well as on the position of the test vehicle within its own lane. Usually rapid changes in the dynamics are not desired for comfort functions and are mainly caused by emergency functions, e.g., the Collision Mitigation System, or malfunctions of the vehicle software. Rapid changes in the dynamics of the test vehicle can be indicators for interventions

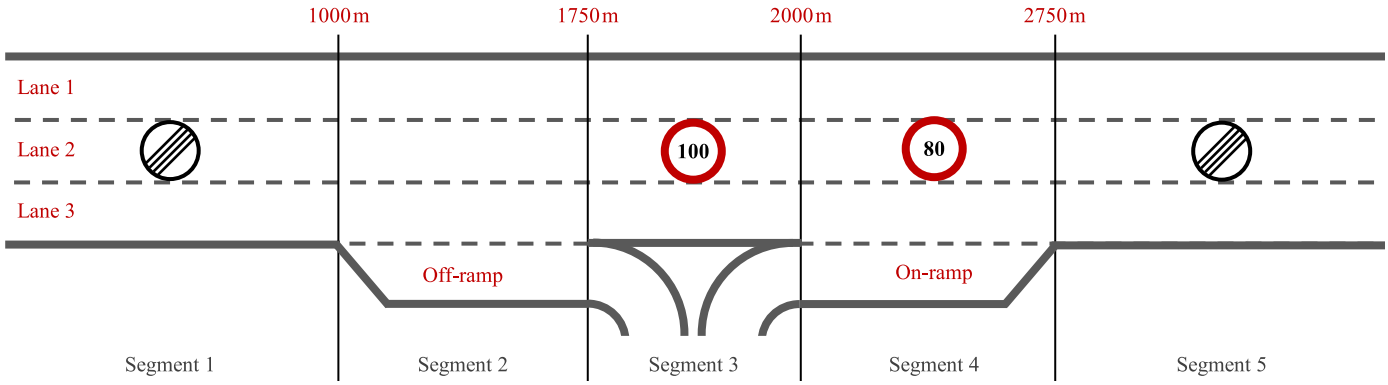

Figure 2. Schematic representation of the road characteristics.

of the automated driving system, which are necessary to prevent collisions with other road users or obstacles. Otherwise, rapid changes can be caused within a certain range to comply with legal requirements, e.g., to maintain the safety distance or the speed limit. Thus, the dynamic behavior of the test vehicle is used to define the metric for how the automated driving system copes with the traffic situation. If an unusual behavior of the test vehicle is found at the system-level, further efforts are necessary to ensure that the traffic situation is within the operating limits of the automated driving system and, if this is confirmed, to find the cause of the issue at lower levels.

IV. Case Study

In this section, an example that was done as a case study is discussed to show the idea behind the presented approach to determine the environmental conditions by evaluating the data captured during a simulated test drive.

A. Generation of the Test Drive Data

The test drive data for the evaluation was generated with a microscopic traffic simulator [15] that provides different car-following and lane-changing models. For the other road users, the "Enhanced Intelligent Driver Model" (ACC) [16] and the "General Lane-Changing Model" (MOBIL) [17] were used, whereas a custom car-following model was implemented for the test vehicle. The car-following model behind the test vehicle has the functionality of an autonomous cruise control system, which maintains a distance to the preceding vehicle on the same lane by automatically adjusting the velocity.

The traffic scenario of the example represents a freeway constructed with five straight road segments, as shown in Figure 2. Each road segment has three lanes by default with the exceptions of the second and the fourth road segment, which have an additional lane on the right side as off-ramp and on-ramp respectively. There are speed limitations in the third and the fourth road segment, which facilitate the lane change of the entering vehicles from the on-ramp lane. Both the off-ramp and the on-ramp cause an increased occurrence of lane changes in their road segments. On the one hand, there is a lower traffic density in the road segment of the off-ramp. On the other hand, there is an increased traffic density in the road segment of the on-ramp. The number of vehicles entering the freeway is

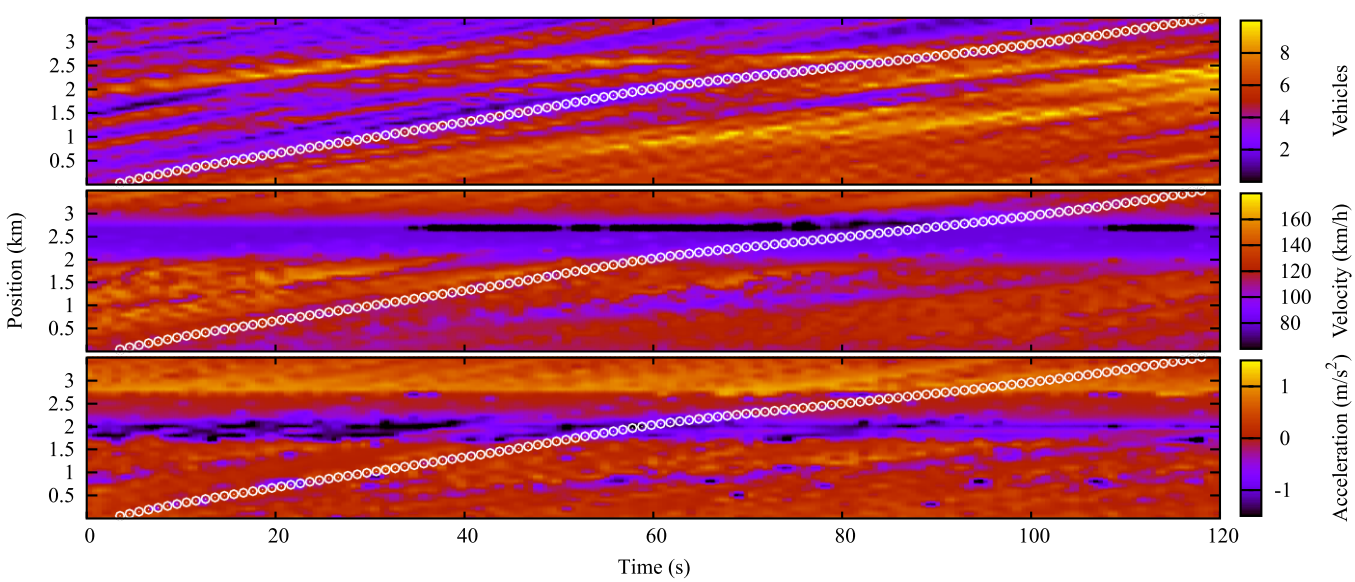

Figure 3. Spatio-temporal diagrams of density, velocity and acceleration including the trajectory of the test vehicle.

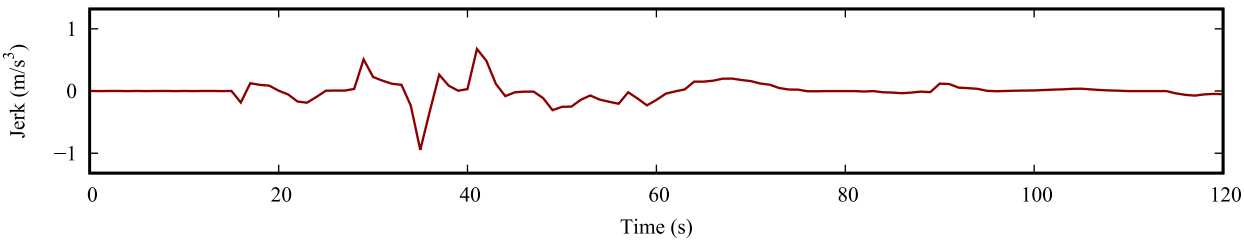

Figure 4. Jerk of the test vehicle during the test drive.

determined by the inflow rate of the traffic simulation. Based on the traffic composition configuration, previously defined vehicle classes are created, which can differ in the parameter set used for the simulation. Overall, there are two classes of vehicles used in the example, a slower and a faster one.

B. Applying the Approach

According to the presented approach, the spatio-temporal context of the captured test drive is firstly analyzed to obtain an overview, in this case an all-knowing overview due to the simulated test drive, about the encountered traffic situations. The spatio-temporal context, as visualized in Figure 3, shows an increasing of the vehicle density over the entire freeway with advancing time in the density diagram, and the speed limitations and the resulting backlog of the traffic with an aggregated velocity, lower than the specified speed limitation in the velocity diagram. The acceleration diagram finally shows road sections on the freeway, where there was a strong acceleration or deceleration of the road users. The position of the test vehicle and its sensor range are simply marked as a circle in the three diagrams, whose area represents the surroundings of the test vehicle and thus the environmental conditions processed by the automated driving system. Since the example is a straight road, the color within the circles of the density diagram illustrates the value of the complexity metric.

The evaluation is continued with an analysis of the movement of the test vehicle. Based on the jerk, as displayed in Figure 4, points of interest are searched in the test drive with an absolute value greater than a specified limit, on which a closer look could be worthwhile. At time 35 s, a significant change in the signal sequence of the jerk occurred followed by a reaction in the opposite direction only a few seconds later. In the remaining time, the value of the jerk changes only slightly. The significant change can be an indicator for an intervention of the automated driving system to prevent a collision.

Finally, the environmental conditions encountered during the test drive are analyzed to check whether a reaction of the automated driving system was necessary and if it was within the specified limits. For this purpose, Figure 5 shows the objects within an assumed sensor range of 100 m ahead of the test vehicle for each lane of the freeway. The color of an object represents the relative approaching between the test vehicle and the object. The object comes closer with a positive value and moves away with a negative value. A trajectory of an object starts after entering a sensor range of the test vehicle at a specific lane. The trajectory ends, if the object leaves the sensor range of the test vehicle or after a lane change. After a lane change within the sensor range, the trajectory has to start at the new lane. In the example, only the third lane has a relevance to the movement of the test vehicle when driving straight ahead.

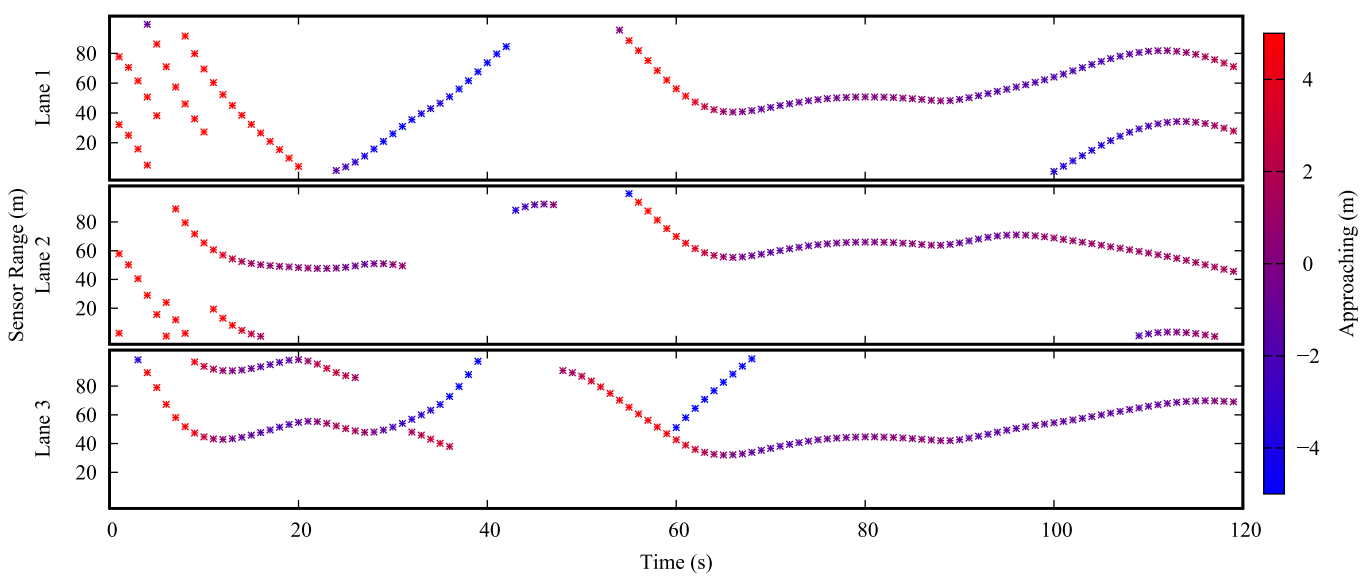

Figure 5. Objects within the sensor range of 100 m ahead of the test vehicle separated by lanes.

The analyzed data shows that the point of interest was caused by a lane change of a road user, who wanted to leave the freeway at the off-ramp. For this purpose, the road user has used the safety gap between the test vehicle and the preceding road user to move from the second lane to the third lane and at last to the off-ramp. Therefore, the automated driving system slowed down the test vehicle to restore the safety distance. At the point of interest, the value for the criticality metric is high due to the fast approaching of the preceding road user on the same lane as the test vehicle. After the road user had left the freeway, the test vehicle was able to strongly accelerate.

V. Conclusion and Future Work

The paper has discussed that robustness testing is necessary to ensure a safe operation of an automated driving system within different environmental conditions. With reaching the driving automation level ”Conditional Automation”, the full responsibility for the vehicles and possible damages lies with the automobile manufacturers until the takeover of the vehicle control by the human driver. The warning period for the handover will increase due to the allowed distraction of the human driver towards the surroundings of the vehicle. This means that the automated driving system must never get into a state, starting from its activation to the completion of the handover, in which the human driver is needed to cope with a traffic situation. In contrast to the currently performed testing, which only show that the human driver is rarely needed as an immediate fallback level, the testing for those systems should cover the spectrum of possible traffic situations.

It has been shown that the presented approach contributes to the testing of automated driving systems. Based on the evaluation of the test drive data, the environmental conditions can be determined and further analyzed. The analysis provides metrics about the environmental conditions, from which the complexity and the criticality of the traffic situations can be derived. The approach can be used with both data from real test drives and with data obtained from simulations. Therefore, it must be taken into account that the data captured during a real test drive can be inaccurate and incomplete, and data recorded from the simulation might be not realistic. A sufficient imitation of the real-world system is supposed to be precise enough for the simulation, so that it is usually not necessary to consider all eventualities in the simulation.

It is left for future work to evaluate, how significant the determined environmental conditions and the derived metrics are, and how the approach can be integrated in the development process. Particularly in the field of testing, application areas are seen in the search for comparable traffic situations, in the detection of software areas that have not yet been tested and thus to track the progress of the testing, as well as in the test optimization to contribute to an effective testing. In the next step, the approach shall be used to evaluate traffic situations of a staged test drive captured from a real test vehicle to compare the determined and the real environmental conditions.

References

[1] Federal Statistical Office of Germany, “Road Traffic Accidents - 2015 (”Verkehrsunfälle - 2015”),” 2016, [Online]. Available: https://www.destatis.de/DE/Publikationen/Thematisch/TransportVerkehr/Verkehrsunfaelle/VerkehrsunfaelleJ2080700157004.html [retrieved: March, 2017].

[2] D. Rösler, “The relevance of traffic elements in driving situations definition, measurement, and application,” Ph.D. dissertation, Chemnitz University of Technology, 2010. [Online]. Available: http://nbn-resolving.de/urn:nbn:de:bsz:ch1-201000403

[3] NHTSA’s National Center for Statistics and Analysis, “Critical Reasons for Crashes Investigated in the National Motor Vehicle Crash Causation Survey,” 2015, [Online]. Available: https://crashstats.nhtsa.dot.gov/Api/Public/ViewPublication/812115 [retrieved: March, 2017].

[4] Federal Statistical Office of Germany, “About Us - Federal Statistical Office (Destatis),” 2017, URL: https://www.destatis.de/EN/AboutUs/AboutUs.html [retrieved: March, 2017].

[5] Verband der Automobilindustrie e.V., “Automation - From Driver Assistance Systems to Automated Driving,” 2015, [Online]. Available: https://www.vda.de/dam/vda/publications/2015/automation.pdf [retrieved: March, 2017].

[6] SAE International, “Automated Driving - Levels of Driving Automation are Defined in New SAE International Standard J3016,” 2014, [Online]. Available: https://www.sae.org/misc/pdfs/automated_driving.pdf [retrieved: March, 2017].

[7] Gesamtverband der Deutschen Versicherungswirtschaft e.V., “Takeover times in highly automated driving - Compact accident research,” 2016, [Online]. Available: https://udv.de/en/publications/compact-accident-research/takeover-times-highly-automated-driving [retrieved: March, 2017].

[8] S. Ulbrich, T. Menzel, A. Reschka, F. Schuldt, and M. Maurer, “Defining and Substantiating the Terms Scene, Situation, and Scenario for Automated Driving,” in 2015 IEEE 18th International Conference on Intelligent Transportation Systems, Sept 2015, pp. 982–988. [Online]. Available: https://doi.org/10.1109/ITSC.2015.164

[9] Fraunhofer Institute for Industrial Engineering IAO, “Highly Automated Driving on Freeways - Industrial Policy Conclusions (”Hochautomatisiertes Fahren auf Autobahnen Industriepolitische Schlussfolgerungen”),” 2015, [Online]. Available: http://www.bmwi.de/Redaktion/DE/Downloads/H/hochautomatisiertes-fahren-auf-autobahnen.html [retrieved: March, 2017].

[10] S. Wittel, D. Ulmer, and O. Bühler, “Challenges in Functional Testing on the Way to Automated Driving,” in The Twelfth International Conference on Systems, 2017.

[11] H. Winner, W. Wachenfeld, and P. Junietz, “Safety Assurance for Highly Automated Driving The PEGASUS Approach,” 2016, [Online]. Available: http://www.fzd.tu-darmstadt.de/media/fachgebiet_fzd/publikationen_3/2016_5/2016_Wi_Wf_Ju_TRB_AUVSI_AVS_San_Francisco.pdf [retrieved: March, 2017].

[12] M. Treiber and A. Kesting, Traffic Flow Dynamics. Berlin, Heidelberg: Springer Berlin Heidelberg, 2013, pp. 7–24. [Online]. Available: http://dx.doi.org/10.1007/978-3-642-32460-4

[13] S. Wittel, D. Ulmer, and O. Bühler, “Automatic Test Evaluation for Driving Scenarios Using Abstraction Level Constraints,” in The Eighth International Conference on Advances in System Testing and Validation Lifecycle, 2016, pp. 14–19. [Online]. Available: http://www.thinkmind.org/index.php?view=article&articleid=valid_2016_2_20_40023

[14] R. Kosinski and R. Stepien, “Simple quantitative analysis of spatio-temporal diagrams for domain wall dynamics,” Acta Physica Polonica A, vol. 87, no. 3, pp. 575–583, Mar 1995. [Online]. Available: http://przyrbwn.icm.edu.pl/APP/PDF/87/a087z3p02.pdf

[15] M. Treiber and A. Kesting, “An Open-Source Microscopic Traffic Simulator,” IEEE Intelligent Transportation Systems Magazine, vol. 2, no. 3, pp. 6–13, Fall 2010. [Online]. Available: https://doi.org/10.1109/MITS.2010.939208

[16] A. Kesting, M. Treiber, and D. Helbing, “Enhanced intelligent driver model to access the impact of driving strategies on traffic capacity,” Philosophical Transactions of the Royal Society of London A: Mathematical, Physical and Engineering Sciences, vol. 368, no. 1928, pp. 4585–4605, 2010. [Online]. Available: http://rsta.royalsocietypublishing.org/content/368/1928/4585

[17] M. Treiber and A. Kesting, Modeling Lane-Changing Decisions with MOBIL. Berlin, Heidelberg: Springer Berlin Heidelberg, 2009, pp. 211–221. [Online]. Available: http://dx.doi.org/10.1007/978-3-540-77074-9_19

Measuring Safety in Aviation: Empirical Results about the Relation between Safety Outcomes and Safety Management System Processes, Operational Activities and Demographic Data

Steffen Kaspers, Nektarios Karanikas, Selma Piric,
Robbert van Aalst, Robert Jan de Boer
Aviation Academy
Amsterdam University of Applied Sciences
Amsterdam, The Netherlands
Email: s.e.kaspers@hva.nl, n.karanikas@hva.nl,
s.piric@hva.nl, r.j.aalst@hva.nl, rj.de.boer@hva.nl

Alfred Roelen
Safety Institute
Netherlands Aerospace Centre
Amsterdam, The Netherlands
Email: alfred.roelen@nlr.nl

***Abstract*— A literature review conducted as part of a research project named "Measuring Safety in Aviation – Developing Metrics for Safety Management Systems" revealed several challenges regarding the safety metrics used in aviation. One of the conclusions was that there is limited empirical evidence about the relationship between Safety Management System (SMS) processes and safety outcomes. In order to explore such a relationship, respective data from 7 European airlines was analyzed to explore whether there is a monotonic relation between safety outcome metrics and SMS processes, operational activity and demographic data widely used by the industry. Few, diverse, and occasionally contradictory associations were found, indicating that (1) there is a limited value of linear thinking followed by the industry, i.e., "the more you do with an SMS the higher the safety performance", (2) the diversity in SMS implementation across companies renders the sole use of output metrics not sufficient for assessing the impact of SMS processes on safety levels, and (3) only flight hours seem as a valid denominator in safety performance indicators. At the next phase of the research project, we are going to explore what alternative metrics can reflect SMS/safety processes and safety performance in a more valid manner.**

Keywords - Safety Metrics; Safety Management Systems; Safety Performance; Safety Outcomes.

I. INTRODUCTION

This paper presents part of an on-going 4-year research project "Measuring Safety in Aviation – Developing Metrics for Safety Management Systems" [1] executed by the Amsterdam University of Applied Sciences and co-funded by the Nationaal Regieorgaan Praktijkgericht Onderzoek SIA [2]. A literature review we conducted in 2016 identified several challenges concerning the measurement of safety [3]. Between February and June 2016, surveys were executed to explore (1) what, how and why, safety metrics are used and (2) whether a monotonic relation between Safety Management System (SMS) process metrics and safety outcomes could be established.

Safety outcomes are defined as accidents, (serious) incidents, occurrences and other safety related events [3]. SMS process metrics include indicators on safety staff, improvements, training, communication, hazard identification, risk management and emergency response [3]. A full listing is given in appendix 2. The SMS process metrics can be applied at a system level but are usually more informative at the sub-system (department, activity type etc.) level. Safety outcomes on the other hand are emergent indicators representative of the whole system.

The results from the first part of the surveys were presented in the International Cross-industry Safety Conference 2016 and published in the proceedings [4], thus this paper focusses on the 2nd part of the surveys. The relation between safety related processes and outcomes can be claimed through two channels: empirical evidence or credible reasoning [5]. Since respective empirical evidence is scarce [6], we aimed at finding associations between SMS process and safety outcome metrics by using data collected from the partners of the project.

In section 2, the research problem and the hypotheses are introduced. Section 3 describes the methodology used and the results are presented in section 4. In section 5, the results are discussed. The paper finishes with the conclusion in section 6.

II. RESEARCH PROBLEM

In the literature review [3], it was concluded that the reasoning behind the relationship between SMS processes and safety performance lies principally on linear safety/accident models, where a direct cause-effect relation between safety management activities and safety events is implied. Thus, the relationship between SMS/safety processes and outcome metrics is seen as monotonic in practice under a "necessary but not sufficient" logic; a single failure or deviation from a SMS/safety process might not lead to an adverse outcome, but multiple failures (e.g., malfunctioning barriers) or deviations (e.g., incompliance with procedures) are likely to cause unwanted outcomes. Besides the linear accident models, few systemic models have been introduced in literature [7][8] but they haven't been extensively applied to the industry.

The aforesaid thinking and industry practice are translated into two hypotheses:

Copyright (c) IARIA, 2017. ISBN: 978-1-61208-549-4

H1: There are consistent and similar monotonic relations of SMS process data with safety outcomes across all companies.

In order to judge whether there is a positive or negative effect of an SMS process on safety outcomes, the direction of the relationship, the scope and timeliness of the respective process must be considered. For example, in the cases of safety training and audits, a negative correlation is expected under the argument that more training or audits lead to fewer safety events. When considering other SMS processes, such as safety reporting and hazard identification, a positive correlation might be expected since those activities retrofit risk assessment with a goal to mitigate risks and improve safety performance; on the other hand, a negative correlation might also reflect that risk assessment does not succeed to increase safety performance, meaning to decrease adverse events.

H2: There are consistent and similar monotonic relations (i.e., regardless their positive or negative direction) of demographic and operational activity data with safety outcomes across all companies.

Correlations of operational activity or/and demographic data with safety outcomes (1) over time for each company and (2) across the whole sample when considering respective averages per company, indicate validity of the respective indicators used in the industry (e.g., accidents per passenger miles or flights).

III. METHODOLOGY

Thirteen companies who participated in the project were asked to provide data in the form of a data-sheet. The request was based on the types of metrics identified through the literature [3] and represented in appendices 1 and 2. The data sheet included 5 operational activity figures (e.g., departures), 12 demographic data fields (e.g., number of staff,), safety outcomes (e.g., number of occurrences of various severities) and 38 fields covering output and frequency of SMS activities (e.g., number of hazards identified, amount of SMS documentation updates) from up to 10 years. Specific instructions were not provided since the fields correspond to data that organizations are familiar with, but some clarifications were offered upon request from the partners.

Ten companies provided the data requested within the time frame set. Most of the large companies reported that they needed considerable time and resources for retrieving the data from several databases since such data were not always directly linked to safety performance and maintained by the safety department. Two large companies sent their annual safety dashboards and the research team converted that data to the respective fields of the datasheet. Due to a recent implementation of a SMS in three out of the ten companies, the sheets received did not include enough data points for statistical analysis. Consequently, data sets from seven companies were used for statistical tests (Table 1).

TABLE 1: RESEARCH SAMPLE

	Size		Domain			
	Large (N=7)	Small (N=6)	Flight Ops (N=7)	ATC (N=2)	GS (N=1)	MRO (N=3)
Data-sheets	2	3	4	1		
Dash-boards	2		1	1		
Insuffi-cient data	1	2	1		1	1

After the collection of data, raw figures were converted to ratios in order to use comparable figures across years for each company; this resulted in an extensive list of measures. The researchers tested all available pairs (i.e., Operational Activities – Outcomes, Demographics – Outcomes and SMS processes – Outcomes) as a means to examine all relationships. Because of the limited sample size, all data were tested with non-parametric correlations. Spearman's coefficient was chosen to explore any monotonic relations of SMS/operational/demographic metrics with safety outcome ones. Spearman's coefficient indicates the presence of a monotonic relationship and not the strength of linear associations. The statistical significance was set to p=0.05.

IV. RESULTS

Table 2 shows the number of pairs tested for monotonic relations. The table is divided into three sections corresponding to operational activities, demographics and SMS processes tested for associations with safety outcomes.

TABLE 2: VALID PAIRS TESTED FOR MONOTONIC RELATIONS

	Operational Activities - Outcomes		Demographics - Outcomes		SMS - Outcomes	
Company	Valid pairs	Significant correlations	Valid pairs	Significant correlations	Valid pairs	Significant correlations
1	4	0, (0%)	0	0, (0%)	25	0, (0%)
2	30	6, (20%)	57	7, (12.3%)	165	19, (11.5%)
3	3	0, (0%)	0	0, (0%)	12	5, (41.7%)
4	36	10, (27.8%)	0	0, (0%)	116	27, (23.3%)
5	232	0, (0%)	188	6, (3.2%)	1292	82, (6.3%)
6	62	8, (12.9%)	48	20, (41.7%)	380	42, (11.1%)
7	72	57, (79.2%)	12	8, (66.7%)	12	8, (66.7%)
Total	439	81 (18.5%)	305	41 (13.4%)	2002	183 (9.1%)

Copyright (c) IARIA, 2017. ISBN: 978-1-61208-549-4

TABLE 3: CORRELATION OF AVERAGES OF ACTIVITY/DEMOGRAPHIC DATA WITH SAFETY OUTCOMES

Demographic and Operational Activity Figures (Averages of Companies)	Safety outcomes			
	Serious Incidents	Incidents	Occurrences	All Events
Flight Hours	$r_s(6)=0.845$ $p = .034$		$r_s(5)=0.900$ $p = .037$	$r_s(6)=0.943$ $p = .005$
Full Time Equivalent of Contractors		$r_s(4)= -1.000$ $p = .000$		
Flight Hours per Pilot			$r_s(3)=1.000$ $p = .000$	$r_s(3)=1.000$ $p = .000$

Within each section, the number of valid pairs are mentioned and the significant correlations for those pairs of data [number, (percentage)].

Appendix 3 includes a sample of cases where significant correlations within companies were found; the whole set of results were published in a technical report [9]. The cells in the corresponding tables include the direction of each correlation (i.e., POS: Positive and NEG: negative) and the number of companies for which the data permitted the conduction of valid correlations per case (i.e., sample N). The cells where POS or NEG are followed by a number (i.e., x Number) indicate how many companies had the respective significant correlation.

In addition to the results within companies, Table 3 shows the significant correlations of the averages of safety outcomes of all severities with activity (e.g., departures) and demographic data (e.g., full time equivalent of company staff,). Tests for miles flown were not feasible due to limited data. Through those correlations, we explored the validity of using demographic or operational activity data as denominators of ratios of adverse safety events, since such ratios are used by the industry to measure safety performance.

The findings presented in Table 3 showed that:

- Increased flight hours' activity is associated with more occurrences, serious incidents and safety events in general.
- The more FTEs are spent by contractors, meaning the more the outsourcing of company activities, the fewer the incidents recorded by the company.
- The more the flight hours' load per pilot, the more the occurrences and events in general.

Taking into account that the flight hours was the main variable associated with some types of safety outcomes, we conducted further statistical tests as follows (table 4):

- Mann – Whitney test was used as a means to explore if the ratios of each event type by flight hours differ between large companies and SMEs. The calculations did not show significant differences.

TABLE 4: DIFFERENCES BETWEEN AND WITHIN LARGE COMPANIES AND SMES.

Event type / flight hours	Mann – Whitney test between large companies and SME	Kolmogorov – Smirnov tests between SMEs
Accident	p=0.690	p=0.001
Serious Incident	p=0.143	
Incident	p=0.095	p=0.049
Occurrence	p=0.800	
All events combined	p=0.133	

- Kolmogorov - Smirnov tests were conducted for the ratios of each event type by flight hours for SMEs; the sample size did not allow the conduction of those tests for large companies. The results showed significant differences between SMEs regarding accidents and incidents per flight hours.

V. DISCUSSION

According to the results, the following observations can be made:

1. The significant correlations regard only part of the SMS processes and safety outcomes and a small portion of the sample, and the distribution of associations is highly scattered. No strong evidence was found that the output and frequency of all SMS processes had an effect on safety outcomes; significant associations were found only for few of the participant companies.
2. The results suggest that just the operation of an SMS does not guarantee an effect on safety outcomes; therefore, that other factors, such as the quality of SMS processes, might play an important role. Also, an evaluation of the effectiveness of an SMS against high severity events seems unjustified in the frame of this survey. More specifically:

a. Most of the significant correlations were found for occurrences (i.e., the lowest severity category of safety events) as well as all safety outcomes regardless their severity.

b. Accidents, serious incidents and incidents and their ratios by activity and demographic figures were associated with a very few SMS processes.

c. Only at a few companies the outputs and frequency of SMS processes had a visible effect on low severity events, the latter reflecting safety performance at shorter intervals.

3. There were 33 negative and 124 positive correlations between SMS process and safety outcomes. However, in 59 cases of all correlations the data regard a single company that provided respective data, so the results cannot be deemed as representative of the whole sample. Nevertheless:

a. The negative correlations sporadically regarded numbers or ratios related to staffing of the safety department, internal audits, safety training, safety surveys and hazard identification. Although due to the limited sample those associations cannot be generalized, the aforementioned areas of SMS processes were influential on safety outcomes of low severity mostly for a single company. It is noticed that a negative correlation between SMS processes and safety outcomes can be considered as a positive case only when outcomes decrease over time; in case that, under a negative

correlation, events increase over time, the SMS can be contemplated as insufficient.

b. Most of the positive correlations were found for the safety reporting and risk assessment processes, the interpretation of those associations being dependable on the timeliness of those processes. The SMS activities are performed continuously, so a distinction between a "positive reactiveness" (e.g., more risk assessments occur due to more outcomes) and "negative proactiveness" (e.g., more risk assessments lead to an increase of adverse events) is not directly evident. Contextual information is of paramount importance in order to interpret such results correctly.

Observation No 1 suggest that hypotheses H1 is partially rejected due to the limitations imposed by the sample size. Additionally, the diverse ways that SMS processes are implemented across the industry and over time, and the different interpretations of outcome thresholds [9] might have affected the results and the validity of comparisons within and amongst companies.

A. *Correlations between operational activities and safety outcomes*

The results presented in Appendix 3 do not suggest a consistent picture within companies. Some activity data related to departures, miles flown and flight hours were associated with all safety events, incidents and serious incidents, but in the majority of the cases those findings regarded only one company out of the whole sample. Only in seven cases the associations of flight hours related data with some types of safety outcomes were found for two companies. Interestingly, accidents were not represented in the significant correlations with operational activities, although annual reports published by regional and international bodies use rates of accidents as a means to depict safety performance (e.g., [10]); perhaps, the large sample that such reports include might render the use of accident ratios meaningful, but the results of our survey showed that those ratios might not be representative of safety performance at the company level. The latter is also supported by the fact that we did not observe any association between operational activity data and number of accidents when considering averages across the sample (Table 3).

Furthermore, in the case of flight hours, the correlations with outcomes were found interchangeably positive or negative depending on the denominator and the company, whereas in few cases the same correlation was found negative for one company and positive for another. This observation might once more reflect the dissimilarities in the interpretation of safety outcome definitions, or/and the differences regarding the effectiveness of safety management in those companies; a positive correlation between activity and outcome data indicates that safety management is not improving (i.e., as safety management activities increase, safety outcomes increase too and vice versa), whereas a negative correlation signals that safety management performs either as expected (i.e., when outcomes decrease over time) or poorly (i.e., when outcomes increase over time).

Monotonic relations were found across the companies regarding flight hours and flight hours per pilot with safety outcomes, the accidents excluded, thus suggesting that the specific type of operational activity might be a more valid exposure measurement than departures and miles flown. By nature, departures do not reflect the total load imposed to company staff (e.g., time that pilots fly or maintenance requirements based on the hours that aircraft operate), and miles flown are not also directly related to the total load due to a variety of factors such as aircraft capabilities, flight plans and fuel efficiency policies (e.g., the same distance might be covered in shorter or longer time based on the air traffic and average flying speed). The findings of our study are aligned with [11], who showed a relation of task load expressed in total flight hours per employee with rates of events attributed to human error.

B. *Correlations between demographics and safety outcomes*

The picture is even more distorted regarding the relationship between demographic figures and safety outcomes. The correlations found were highly dependable on the denominators used in the safety outcomes; for example, the average aircraft age was positively correlated with number of occurrences and the ratio of occurrences by flight hours, but negatively correlated with the ratios of occurrences by miles flown and departures. Hence, under the expectation that the higher the age of the aircraft, the more the occurrences under increasingly complex operations, it seems that, in this case too, flight hours can act as a more representative denominator compared to miles flown and departures.

Furthermore, the number of company employees was positively correlated with occurrences, but negatively associated with incidents and all safety events regardless severity. Although those differences do not refer to the same company, they suggest that the use of raw demographic data alone cannot render respective indicators valid. In conjunction with the discussion of the results of the paragraph above, ratios of activity figures, and especially flight hours, by demographic data can be more valid representations of risk exposure in comparison with net numbers of operational activities or demographics.

Taking into account the overall picture and the limitation imposed by the sample size, the researchers claim that the hypothesis H2 is partially rejected. As in the discussion of the hypothesis H1, the different interpretations of outcome thresholds might have affected the results.

VI. CONCLUSIONS

From the numerical analysis of the data sample, consistent correlations between operational activity figures, demographic data, SMS process data and safety outcomes could not be established. The correlations in the sample demonstrated a wide variety, and there were no correlations supported by all usable datasets. Only part of the datasets resulted to significant correlations for specific combinations of data, and in some cases, there were both positive and negative correlations for the same pair of variables in the sample.

Due to the limited sample size (i.e., number of participating companies and data points per company), we do

not claim external validity of the results and we could not fully reject the research hypotheses. However, since the latter cannot be fully confirmed, the current practices in safety performance measurement seem of limited validity. The partial rejection of hypotheses H1 and H2 is aligned with, and indirectly validated by, the concerns of the companies about the existing safety metrics and their needs for better / alternative ones [9]. Nevertheless, the diverse and, occasionally, contradictory findings from the quantitative analysis might be attributed to the (1) different interpretations of thresholds of safety outcomes, (2) implementation of SMS processes in various ways, due to which the data points of this study reflected different contexts of the companies and changes over time, and (3) limited value of the linear approach to safety, as suggested by the models widely used by the industry and the emergent behavior at the system level that constitutes safety. This latter consideration is exuberated by the mismatch of indicators at the sub-system (department, activity process) and system level.

In overall, the findings of this study indicate the need to move towards the development of metrics that will be more representative of SMS processes and safety outcomes and will allow valid comparisons over time and across the industry. Based on the results of this research phase, the justification of the overall project does not only stem from a need to improve scientific knowledge on the topic of aviation safety metrics, but it is also jointly supported by the concerns and needs of the industry and the findings of the analysis of numerical data collected in this research phase.

ACKNOWLEDGMENT

The research team would like to expresses their deep thanks to:

The companies which participated in the surveys: Helicentre, KLM (Royal Dutch Airlines), KLM Cityhopper, Life Line Aviation, LNVL (Air Traffic Control the Netherlands), MUAC (Maastricht Upper Area Control Centre), Olympus Airways, SAMCO, Sky Service Netherlands, Transavia.

The members of the knowledge experts group of the project, who reviewed and provided enlightening and valuable feedback (in alphabetical ascending order of partner organization): CAA NZ: C. Mills, EASA: J. Franklin, Kindunos: J. Stoop, KLM Cityhopper: E. Hiltermann, Klu / MLA: R. Van Maurik, Purdue University: J. Keller, Team HF: G. Hofinger, TU Delft: A. Sharpanskykh.

REFERENCES

[1] Aviation Academy. “Project Plan RAAK PRO: Measuring safety in aviation – developing metrics for Safety Management Systems”, Hogeschool van Amsterdam, Aviation Academy, The Netherlands, 2014.

[2] SIA. “Decision on request grant scheme RAAK PRO 2014 for the project Measuring Safety in Aviation - Developing Metrics for Safety Management Systems "(project number: 2014-01-11ePRO)" (“Besluit inzake aanvraag subsidie regeling RAAK-PRO 2014 voor het project Measuring Safety in Aviation – Developing Metrics for Safety Management Systems ' (projectnummer:2014-01-11ePRO)”.) Feature: 2015-456, Nationaal Regieorgaan Praktijkgericht Onderzoek SIA. The Netherlands, 2015.

[3] S.E. Kaspers, N. Karanikas, A.L.C. Roelen, S. Piric, and R.J. de Boer, “Review of Existing Aviation Safety Metrics, RAAK PRO Project: Measuring Safety in Aviation,” Project S10931, Aviation Academy, Amsterdam University of Applied Sciences, the Netherlands, 2016.

[4] S.E. Kaspers et al., “Exploring the Diversity in Safety Measurement Practices: Empirical Results from Aviation”. The First International Cross-industry Safety Conference, Amsterdam, 3-4 November 2016, Journal of Safety Studies, 2(2), pp. 18-29, 2016. DOI: 10.5296/jss.v2i2.10437

[5] J. Wreathall, “Leading? Lagging? Whatever!”. Safety Science, 47(4), 493 – 494. doi:10.1016/j.ssci.2008.07.031

[6] T. Reiman, and E. Pietikäinen, “Leading indicators of system safety – monitoring and driving the organizational safety potentia l.” Safety Science, 50(10), 1993- 2000, 2012. doi:10.1016/j.ssci.2011.07.015

[7] E. Hollnagel, “FRAM, the functional resonance analysis method: modelling complex socio-technical systems,” Ashgate Publishing, Ltd., 2012.

[8] N. Leveson, “Engineering a safer world: Systems thinking applied to safety,” Mit Press, 2011.

[9] S.E. Kaspers, N. Karanikas, A.L.C. Roelen, S. Piric, and R.J. De Boer, “Results from Surveys about Existing Aviation Safety Metrics, RAAK PRO Project: Measuring Safety in Aviation,” Project S10931, Aviation Academy, Amsterdam University of Applied Sciences, the Netherlands, 2016.

[10] EASA, “Annual Safety Review.” Cologne: European Aviation Safety Agency, 2016.

[11] N. Karanikas, “Correlation of Changes in the Employment Costs and Average Task Load with Rates of Accidents Attributed to Human Error,” Aviation Psychology and Applied Human Factors, 5(2), pp. 104-113, 2015.

APPENDIX 1 – SAFETY OUTCOME , ACTIVITY AND DEMOGRAPHIC METRICS

Activity data
Departures
Miles Flown
Flight Hours
Number of Company Staff
Ratio of Company Staff Turnover
Ground movements
Demographic data
Full Time Equivalent (Company)
Full Time Equivalent (Contractors)
Experience of Flight Crews (Flight Hours)
Hours Flown / Pilot
Experience of Ground Staff (Years)
Aircraft Fleet
Aircraft Age (Years)
Safety Outcomes
Number of All Safety Related Events
Number of Occurrences
Number of Incidents
Number of Serious Incidents
Number of Accidents

Copyright (c) IARIA, 2017. ISBN: 978-1-61208-549-4

APPENDIX 2 – SMS PROCESS METRICS

SMS process - Safety Staff
Number of Safety Staff
Full Time Equivalent Safety Staff Spends on SMS
Number of Safety Staff Changed
SMS process - Improvements
SMS updates
SOPs, procedures, rules etc. updates
Number of External Audits
Findings from External Audits
Number of Internal Audits
Findings from Internal Audits
Number of Internal Safety Reviews / Meetings
Days for Implementing Decisions Internal Safety Reviews / Meetings
Number of Safety Meetings with External Organizations
Number of Safety Conferences, Workshops etc. Attended
Number of Safety Surveys
Ratio of Targeted Population Participated in Safety Surveys
Number of Safety Studies Accomplished (in addition to Safety Surveys)
SMS process - Safety Training & Education
Number of Safety Training Sessions Completed
Hours per Safety Training Session
Ratio of Staff Attending Safety Training
Ratio of Staff Passing Safety Training Exams on 1st Attempt
SMS process - Safety Communication
Number of Safety Bulletins, Notices etc.
Times of Safety Communication (each communication might include 1 or more safety messages, posters etc.)
SMS process - Hazard Identification
Number of Safety Reports Submitted by Company and Contractor Staff (e.g., Air Safety Reports, Hazard Reports)
Number of Safety Reports Followed-Up / Feedback Provided
Number of Hazards Identified from Sources Except Safety Reports (e.g., Safety Investigations, Safety Audits, Safety Observations)
SMS process - Safety Risk Assessment & Mitigation
Number of Total Risk Assessments Performed
Number of Risk Assessments Initially Rated as Low
Number of Risk Assessments Initially Rated as Medium
Number of Risk Assessments Initially Rated as High
Number of Risk Assessments Initially Rated as Unacceptable
Number of Low Risks in the Registry (after assessment & mitigation)
Number of Medium Risks in the Registry (after assessment & mitigation)
Number of High Risks in the Registry (after assessment & mitigation)
Days Between Hazard Identification and Risk Assessment
Days Between Risk Assessment & Implementation of Measures
SMS process - Emergency Response
Number of Emergency Response Exercises
Hours Spent on Each Emergency Response Exercise
Number of Emergency Response Planning Updates

Copyright (c) IARIA, 2017. ISBN: 978-1-61208-549-4

APPENDIX 3

	Activity		Demographic			SMS processes										
	Departures	Flight Hours	Number of Company Staff	FTE Company	FTE Contractors	Number of Safety Staff	FTE Safety Staff Spends on SMS	SMS Updates	Number of Internal Audits	Findings from Internal Audits	Findings per Internal Audit	Ratio of Staff Attending Safety Training	Number of Safety Bulletins Notices etc	Number of Safety Reports Submitted by Company and Contractor Staff	Reports Followed Up report submitted	Safety Communication per total staff
Number of All Safety Related Events	6	Pos x 2 5	Pos & Neg 4	Pos 3	2	2	2	3	Pos x 2 3	Pos 4	Pos & Neg 3	Neg 2	3	Pos x 2 3	1	Pos 1
All Safety Related Events per dep		Pos 4	Neg 3	2	1	2	1	2	Pos 3	4	2	1	2	Pos 3	1	Pos 1
Number of Occurences	Pos 4	Pos x 2 4	Pos x 2 3	Pos x 2 3	Pos 2	2	Pos 2	Pos 3	Pos 2	5	Neg 3	2	Pos 3	Pos 3	Pos 1	
Occurences per dep		Pos 3	2	2	1	2	1	1	1	2	1	Neg 1	1	3	1	
Number of Incidents	Pos 5	Pos x 2 4	Neg 3	2	2	1	1	2	Pos 2	3	3	2	2	2	Pos 1	Pos 1
Incidents per dep		Pos x 2 3	Neg 2	1	1	1		1	Pos 2	2	1	1	1	2	1	Pos 1
Number of Serious Incidents	Pos 4	Pos 2	1						2	1				1	1	1
Serious Incidents per dep		Pos 2	1						Pos 1	1				1	1	1
Number of Accidents	1	1	1	1	1	1		1	1	1	1	1	1	1		
Accidents per dep	1	1	1	1	1	1		1	1	1	1	1	1	1		

ERTMS Challenges for a Safe and Interoperable European Railway System

Katja Schuitemaker
Design, Production and Management Department,
University of Twente
Enschede, the Netherlands
email: k.schuitemaker@utwente.nl

Mohammad Rajabalinejad
Design, Production and Management Department,
University of Twente
Enschede, the Netherlands
email: m.rajabalinejad@utwente.nl

***Abstract*— The European Railway Traffic Management system (ERTMS) aims at replacing the different national train control and command systems in Europe and will serve to make rail transport safer. In order to provide insight into safety developments within the European railway system, the present study evaluates ERTMS at both national and international integral level. For this purpose, the international data from European ERTMS implementations is combined with national data obtained from interviews with Dutch ERTMS stakeholders and safety experts. Effects of deregulation, dynamic specifications, interoperability and time drain make that allowing an interoperable railway system by implementing ERTMS appears not to be self-explanatory. Also, without an overarching process, cross-discipline understanding and improved ascribing meaning to data, implementing ERTMS does not mean the railway system will become safer.**

Keywords - ERTMS; safety; integral assessment; socio-technical safety.

I. INTRODUCTION

As early as the 1990s, the European Commission (EC) decided passenger trains should be able to travel across international borders in Europe. In 1998, the EC requested the foundation of the Union Industry of Signalling (UNISIG) and assigned this with the task of drafting technical specifications of the European Railway Traffic Management System (ERTMS). ERTMS was designed to be fully interoperable across the European Union and has become the European standard for the Automatic Train Protection (ATP) that allows an interoperable railway system in Europe.

The International Union of Railways states that the goal of ERTMS is “to enhance cross border interoperability and signalling procurement by creating a single Europe wide standard for railways with the final aim of improving competitiveness of the rail sector” [1]. According to the EC, ERTMS is a project which will serve to make rail transport safer [2]. Some explanations on why ERTMS is considered to increase railway safety include:

- Continuous supervision of the train speed [2]. This means that the train can receive authorization to continue running at maximum allowed speeds continuously through the GSM-R system (only available at ERTMS level 2).
- Reduce the risk for human errors [3]. For example, work related errors caused by stress, sleepiness, fatigue, and sleep disturbance.
- Decreasing the amount of Signals Passed At Danger (SPAD) [4]. This can be explained by the difference with previous ATP systems. ERTMS is able to influence trains driving under 40 km/h.

However, it appears that implementation of ERTMS does not automatically mean a safer railway system. For instance, in practice, in the Netherlands, the amount of SPADs under ERTMS (both Level 1 and Level 2) was 11 in 2013, and 17 in 2015 [5]. Though, these numbers are low, so they can be considered as an indication, not necessarily as a trend. More studies, both scientific and industrial, question the safety level through implementation of ERTMS.

At the international level:

- Smith et al. addresses issues relevant to safe introduction of ERTMS into European railway systems [6]. These issues include technical system integration, technical system failures and human factor considerations.
- Laroche and Guihéry study the European Transport Policy, the role played by the EC, the ERTMS innovation process in accordance with innovation process in surface transport, and the difficulties for the implementation of an intelligent transportation system innovation [7].
- Ghazel addresses the regular evolving documents [8].
- The EC itself has studied past and current problems with ERTMS implementation [9].

At the national Dutch level:

- The Ministry of Infrastructure and the Environment, ProRail and NS have collected (im)possibilities of ERTMS [10].
- ProRail and NS executed a pilot for gaining experience with driving under ERTMS [11].
- A specialized team investigated the sequence of events and decision making processes in the Netherlands, which have led to delays in deployment of the ERTMS train signalling systems in the HSL railway project [12].

Most importantly, ERTMS principles have led to assumptions regarding safety. This paper studies safety implications of ERTMS at the integral level, questioning:

- Assumption 1: the fact that ERTMS aims at *replacing* the different national train control and command systems in Europe [13]. The risk comes from the idea that ERTMS is considered to be a replacing system, instead of a new system with new interfaces in itself.

Copyright (c) IARIA, 2017. ISBN: 978-1-61208-549-4

- Assumption 2: the fact that ERTMS will serve to make rail transport *safer* [2]. This is not self-evident. Parties may gradually sail closer to the wind, thereby unintentionally and unnoticed, compromising too much on safety. Only when things go wrong - as in the Hilversum derailment – it becomes clear that a threshold has been passed [14].

Section 2 provides an overview of the background of railway deregulation, ERTMS specifications, European interoperability, and cost reduction as a result of a change in organisational behaviour. The methodology is discussed in Section 3. Section 4 explains findings with regard to the safety architecture and sociotechnical safety of ERTMS. Findings are discussed in Section 5. Section 6 summarizes, concludes and highlights challenges.

II. BACKGROUND

The railway system includes technical, managerial, organizational, and regulatory aspects. The subsystems can work perfectly individually, but together they can create a hazardous state. Many factors, both technical and socio-institutional in nature should be combined to turn a serious challenge of one European train system into a great success satisfying social needs of lower costs, better utilization of an infrastructure and less complex logistics [15].

A. Deregulation

Starting with the 90s, in order to promote greater competition, the rail industry in Europe was restructured. On one hand, the vertical separation means management and ownership of infrastructure are totally separated from other rail activities. On the other hand, various operators are using infrastructures. Deregulation is the reduction or elimination of government power in industry, usually enacted to create more competition within the industry. In addition, safety regulation has increased a hundred-fold between 1947 and 2008 [16]. At last, the ERA explains a shift from quantitative safety data to qualitative safety data [17].

The privatization and deregulation has led to an increased involvement of private actors, national and international [18].

B. ERTMS specifications

The Union Industry of Signalling (UNISIG) was founded in 1998/99 at the specific request of the European Commission (EC) [19]. It was created to develop ERTMS specifications. The final version of ERTMS specifications is published by the EC following the approval of the Member States.

In November 2012, the EC intentionally deleted ERTMS Functional Requirement Specifications making these specifications no longer mandatory. The remaining System Requirements Specifications are written in natural language, which allows multiple interpretations [20].

C. Interoperability

The meaning of interoperability is two-fold. On one hand, interoperability refers to a geographical interoperability between countries and between projects. On the other hand, it also refers to interoperability between suppliers. This opens the supply market and increases competition within the industry [21]. The result of this is the absence of a single entity that is responsible for the railway system as a whole.

D. Cutting cost and time

Dutch national safety goals are approached through use of the As Low As Reasonably Practicable-principle (ALARP) and standstill-principle [22]. For risks in the “ALARP area”, all potential risk reducing measures must be evaluated in terms of cost efficiency, cost-benefit balance or some similar economic measure. Finally, selected risk-reducing measures may be introduced based on experience or best practice in combination with cost-efficiency considerations [23].

According to Rasmussen [24], systems and organizations continually experience change as adaptions are made in response to local pressures and short-term productivity and cost goals. Several accidents such as Bhopal, Flixborough, Zeebrugge, and Chernobyl demonstrate that they have not been caused by a coincidence of independent failures and human errors, but by a systematic migration of organisational behaviour toward accident under the influence of pressure toward cost-effectiveness in an aggressive, competitive environment. There happens to be a standing request to be cost-effective in risk management [25]. According to the ERTMS strategy group of Great Britain, initially the principal requirement for ERTMS was to improve safety. “Over approximately the last ten years, capacity became a more significant influence and then, more recently, cost reduction [26].”

III. METHOD

In order to investigate the nature of phenomena, a qualitative approach in the form of interviews was executed. The findings in this paper are based on international data from European ERTMS implementations linked with national data obtained from semi-structured interviews with Dutch ERTMS key stakeholders and safety experts from train operating companies, infrastructure managers and self-employers involved with the ERTMS national program. In total, 15 semi-structured interviews have been held, performed face to face, lasting between 30 and 90 min. All interviews were audio recorded and transcribed verbatim.

Emphasis was placed on the ERTMS safety architecture and on social technical safety of ERTMS on both Dutch national and international level. The topics discussed included effects from deregulation, ERTMS specifications, interdisciplinarity and time drain.

Transcriptions were processed through qualitative inductive content analysis in order to develop a theory and identify themes through repeated examination, comparison, abstraction and data reduction. The material was abstracted and reduced to a set of themes. The procedure was repeated to refine chosen themes. Two main categories were identified as a thread through transcriptions: (1) implications with regard

to the safety architecture, (2) implications with regard to socio-technical safety.

IV. FINDINGS

A. Safety architecture

With the implementation of a single signalling system through Europe, the EC has opted for radical innovation for all Member States. Similarly, engineers are often in favour of the most innovative, not yet proven technology [27]. At the same time, instable specifications make it difficult to adopt a radical innovation [7] and issues occur with adapting the new system to the old one. Once a hazard scenario is identified, it is not trivial to identify all the possible causes in the system [28]. In other words, a system that is new, or particularly complex can generate scenarios that are not included in the standard set.

Earlier studies explain that ERTMS specifications are instable [7], [26], written in informal language [8], non-consolidated [6] and incomplete [15], [27]. Up until today, stakeholders indicate specifications are not sufficient. To be more specific, missing parts concern management, integral system integration and physical design.

As a result, updates are postponed in anticipation of new specifications, covering multiple requirements through one update.

For specifications, preferences vary on both international and national level. The signalling system for the trajectory the Netherlands – Germany (remote monitoring) differs significantly from the signalling system for the trajectory the Netherlands – Belgium – France (more autonomy for the train driver, missing track signalling), which is more in line with ERTMS Level 2. Therefore, to migrate to ERTMS Level 2, France does not have to change much. To migrate to ERTMS Level 2, Germany and the Netherlands face a discontinuation with the past. The signal systems as well as the automatic train protection systems are still different from one EU country to the next [28]. In addition, the various ERTMS levels include different technical requirements and applications. A higher level involves less track side equipment, but more on-board equipment. This change also implies that the costs of the signalling system will migrate from infrastructure managers to train operators [12]. Infrastructure managers might anticipate on the developments, where operators do not like to upgrade existing rolling stock [29].

In the same line, various subsystems of the railway system are tendered. At the national level, the 5 ERTMS-projects are explained in table 1.

TABLE I. ERTMS-PROJECTS IN THE NETHERLANDS

Project	Supplier	ERTMS level	In service date
Betuweroute	Alstom	2	2007
Port Rotterdam	Alstom	1	2009
High-Speed Line South	Thales/ Siemens	1/2	2009
Lelystad-Zwolle railway	Alstom	2	2012
Amsterdam-Utrecht railway	Bombardier	1/2	2013

Various ERTMS levels result in multiple transitions. Table 2. shows all the 21 possible transitions between ERTMS levels [31].

TABLE II. ERTMS POSSIBLE TRANSITIONS

From to	0	STM	1	2	3
0					
STM					
1					
2					
3					

In practice, the choice for no nationwide rollout of one ERTMS variation results in many transitions between various subsystems. In other words, realization of implementation is unique for every project, and dependent on stakeholders, environment and activities. As is also explained by Leveson [31], the interconnectivity and interactivity between system components make that greater complexity leads to vastly more possible interactions than could be planned, understood, anticipated or guarded against. In reality, Table II shows just a fraction of the number of transitions. As is also concluded by Smith [6], existence of many ETCS versions with technical problems require the need for a backup system.

As a result, systems can be incompatible, for example, the two implementations made by Alcatel (Dutch part of the railway) and Alstom (Belgium part of the railway).

In the end, with ERTMS, complexity of technology, use, and processes of the railway system increases. Interviewees indicated that the technological development in ERTMS is underestimated. A failure with ETCS can have up to 100 causes where train drivers and signalmen must find a solution through difficult procedures and processes, with limited technical system knowledge.

B. Sociotechnical safety

Deregulation has led to considerably more actors on the market. As is also concluded by [6], incomplete/unstable specifications of ERTMS are further hampered by companies involved. With Dutch automatic train protection (ATB) tracks, only one manufacturer (Alstom) was involved. With ERTMS and the tendering of subsystems, various manufacturers are involved. Stakeholders within the ERTMS program come from, among others operating companies, infrastructure provider and self-employers.

In the first place, the rising number of parties involved entails a considerable amount of points of view, skills, responsibilities and interests to the interaction. Boundaries of what constitutes the system become fuzzy; interdependencies and interactions multiply and mushroom [32]. With so many interests, there is a risk of compromising too much on safety. In this context, the train derailment in Hilversum teaches us that the related interests can gradually and unnoticed apply pressure on the management of safety risks [14].

Copyright (c) IARIA, 2017. ISBN: 978-1-61208-549-4

Second, qualitative data uses subjective indexes and is based on logical reasoning from multiple experts. Differences in both language and culture can be major barriers to multidisciplinary work [33]. On top of this, countries are using their own language, making intersectional issues even more complex. For these reasons, on both international level and national level, stakeholders experience difficulties with understanding their respective system. This is also described by Forsberg [3], who states that the new societal organization indicates that intersectional issues and decisions have increased between the various actors, particularly since mishaps or accidents often are caused by circumstances or weak links between them.

Then, for interoperability, without legal entity, it is difficult for the national ERTMS program to allocate responsibility of interface risks to a stakeholder. What makes this even more difficult, is a missing central designer, or any party, that knows the entire complex system. As is also described by Baxter [33], borders between disciplines have been largely maintained despite efforts at creating interdisciplinary teams by involving domain specialist in the design process. One discipline does not fully understand what other disciplines can do, because it essentially stops after collecting data rather than analysing data to ascribe meaning to it so that it could be more readily used by others. Although the European exposed Common Safety Method (CSM) aims at an integral safety approach, the final report on the ERTMS pilot between Amsterdam and Utrecht explains that "overarching processes between railway and train transportation are missing and that these are necessary for optimum implementation of ERTMS". Employees are often focused on their own job, knowing a lot about their own subject. In practice, data is set and sent to the next. Organizations feel responsible for their own processes, not for the integral railway system as is also recognized by the Dutch Ministry of Infrastructure and the Environment [11].

As it is also described by Nusser [34], "Black box" approaches are regarded with suspicion – even if they show a very high accuracy on the available data – because it is not feasible to prove that they will show a good performance on all possible input combinations. This makes it possible to make a decision based on hidden factors. For example, as safety is sometimes seen as hindrance to effective marketing solutions, focus can be on finishing on time and approve of design.

This is also questioned by Enserink: "It is strange to see how in many large projects, such as the Westerschelde tunnel, the Betuwelijn, and the 'Groene Hart' bored tunnel of the high speed rail line south, the discussions of safety issues and safety management took place at a very late stage in the project cycle" [35]. He also explains: In all the examples in the planning phase, the analysts neglected the safety issues or these issues were temporarily stalled because of their complexity. Many have been investigated with the aim of apportioning blame or liability and although safety recommendations are often made, they frequently fail to identify some of the underlying causes of whatever went wrong [28].

As for time drain, with such a large number of stakeholders, it is not always possible to involve every stakeholder in substantive discussions. As a result, stakeholders try to represent another's perspective. In addition to this, stakeholders are involved in multiple projects resulting in conflicting goals. In other words, the decision-making process can be person related, instead of organization related. According to the parliamentary commission Fyra, it seems like safety has become a subject for negotiation [36]. In practice, the safety case HSL-Z resulted in only mitigating major issues due to time pressure [37].

In the end, any of these effects enable local actors to change their conditions in one of its corners for a very good reason without apparent implications. This can bring immediate gains on some local goal trade-off. Both Leveson [31] and Dekker [32] explain that with a vast number of widely distributed interacting components in an organization, small 'drifts' in procedure or policy will not necessarily be identified as risks to the safety of the SoS. Figure 1 shows the interrelationships between the effects of deregulation, dynamic specifications, interoperability and time drain involved with ERTMS.

V. Discussion

A. Safety architecture

Both internationally and nationally, stakeholders have different preferences for ERTMS design. In addition, specification interpretations by manufacturers vary. This in turn leads to a system of a wide variety of subsystems and the associated increase of transitions. This, whilst the ERTMS program tries to prevent transitions between subsystems [38]. The checking of the critical specifications in the natural language is a burdensome task. At the same time, new trains are designed, without required ERTMS specifications. In practice, the instable specifications and various interpretations are a major issue when dealing with such systems. The consequences are significant: the 5 ERTMS-projects (Betuweroute, Port of Rotterdam, HSL South, Amsterdam-Utrecht and Lelystad-Zwolle) are all different [10], let alone the European variations.

Both international and national preferences, changing specifications, changing stakeholders and varying manufacturers led to a unique realization for every subsystem. Along the same line, the occurrence of further transitions with accompanied complexity and procedures and processes that multiply and have wider ramifications.

To pick up from the assumption that ERTMS *replaces* the national train control and command systems, all in all, it can be concluded that the greater complexity leading to vastly more possible interactions, was and is, unforeseen. As of today, the goal for one interoperable railway system is not achieved. Challenges concern systems thinking accompanied by complex interdisciplinary systems.

B. Sociotechnical safety

With ERTMS and the tender strategy, information has become more sensitive. As a result, stakeholders lack insight into cross-border information. Also, ERTMS involves an

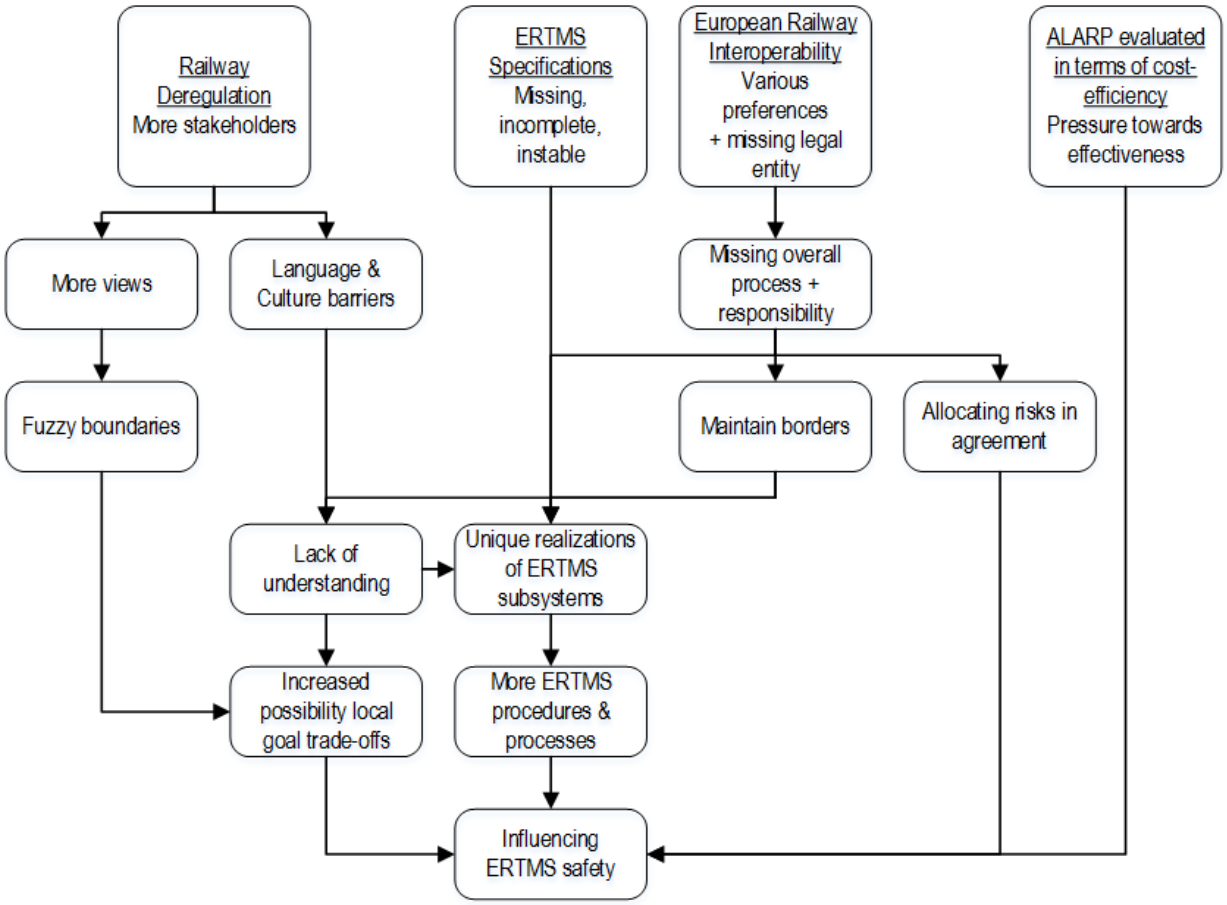

Figure 1. Interrelationships between effects of deregulation, dynamic specifications, interoperability, and time drain of ERTMS.

increased number of stakeholders that differ in both language and culture. As for safety, this means that lack of availability of information makes it difficult to determine a root cause.

A central designer that knows or has the responsibility over the entire complex system misses. This, in combination with stakeholder involvement in multiple projects, make local-goal trade-offs possible. Since there is no integral view, local actors can change their conditions without apparent implications.

Time drain and pressure towards cost-effectiveness can inadvertently lead to generating adaptive responses, wrong/missing identification of hazards and safety risks and also to safety concessions. In the same line, if only catastrophic issues are addressed, many other hazards may go uncorrected, which may have a costly impact.

To pick up from the assumption that ERTMS will serve to make rail transport *safer*, both implicit data-exchange and a missing integral view make it hard to perform a comprehensive safety assessment. Challenges concern the overarching process, cross-discipline understanding and ascribing meaning to data.

VI. CONCLUSION

In present study, the effects of deregulation, dynamic specifications, interoperability, and time drain on the European railway system have been researched.

First, allowing an interoperable railway system by implementing ERTMS appears not to be self-explanatory. Second, implementing ERTMS does not mean the railway system will become safer.

Specifications allowing multiple interpretations result in various design choices, disparities between systems, possible little recognition of hazards and risks, and cumbersome procedures. Realizations are dependent on stakeholders, environment and activities. As of today, the goal for one interoperable railway system is not achieved. Challenges concern systems thinking accompanied by complex interdisciplinary systems. A missing central designer and overall process lower the degree to which the parties succeed in correctly harmonizing various processes. Since there is no integral view, local actors can change their conditions without apparent implications.

As is also concluded by the Dutch Safety Board [39], railway undertakings should make transparent as to why they decide to implement certain measures or not. Challenges

concern the overarching process, cross-discipline understanding and ascribing meaning to data.

REFERENCES

[1] International Union of Railways, "SafeCulture: A method for assessing organisational safety at interfaces," UIC, 2004.

[2] European Commission, "ERTMS – European Rail Traffic Management System," Available from: http://www.ec.europea.eu [retrieved: March, 2017].

[3] R. Forsberg, "Conditions affecting safety on the Swedish railway – Train drivers' experiences and perceptions," Safety Science, vol. 85, pp. 53-59, 2016.

[4] Ministry of Infrastructure and the Environment, "Beleidsimpuls Railveiligheid," 2016 Available from: http://www.rijksoverheid.nl [retrieved: March, 2017].

[5] Prorail, "Jaarrapport 2015. Analyse STS-passages" Unpublished.

[6] P. Smith, A. Majumdar, and W. Y. Ochieng, "An overview of lesson learnt from ERTMS implementation in European railways," Journal of Rail Transport Planning & Management, vol. 2, pp. 79-87, 2012.

[7] F. Laroche, and L. Guihéry, "European Rail Traffic Management System (ERTMS): Supporting competition on the European rail network?" Research in Transportation Business & Management, vol. 6, pp. 81-87, 2013.

[8] M. Ghazel, "Formalizing a subset of ERTMS/ETCS specifications for verification purposes," Transportation Research Part C, vol. 42, pp. 60-75, 2014.

[9] European Commission, "ERTMS – FAQ on ERTMS," Available from: http://www.ec.europa.eu [retrieved: March, 2017].

[10] Ministry of Infrastructure and the Environment, "ERTMS kennisboek versie 2.0," 2014 Available from: http://www.rijksoverheid.nl [retrieved: March, 2017].

[11] Ministry of Infrastructure and the Environment, "Eindrapport Lessen uit het rijden onder ERTMS Level 2 in Dual Signalling omstandigheden," 2015 Available from: http://www.rijksoverheid.nl [retrieved: March, 2017].

[12] J. Stoop, J. Vleugel, and J. Baggen, "Testing the untestable: towards pro-active safety assessment," Proceedings of the 9th International probabilistic safety assessment and management conference (PSAM 9), May 2008, pp. 784-791, ISBN: 978-988-99791-5-7.

[13] UNIFE, "ERTMS in brief," Available from: http://www.ertms.net [retrieved: March, 2017].

[14] The Dutch Safety Board, "Train Derailment Hilversum," 2014 Available from: http://www.onderzoeksraad.nl [retrieved: March, 2017].

[15] L. de Haan, J.L.M. Vrancken, and Z. Lukszo, "Why is intelligent technology alone not an intelligent solution?" Futures, vol. 43, pp. 970-978, 2011.

[16] A. S. Townsend, "Safety Can't Be Measured – An Evidence-based Approach To Improving Risk Reduction," Gower Publishing, 2013.

[17] European Railway Agency, "Intermediate report on the development of railway safety in the European Union," 2013 Available from: http://www.era.europa.eu [retrieved: March, 2017].

[18] G. Alexandersson, and S. Hultén, "The Swedish Deregulation Path,"Review of Network Economics, vol. 7, issue 1, pp. 1-19, March 2008.

[19] UNIFE, "UNISIG, An industrial consortium to develop ERTMS/ETCS technical specifications," Available from: http://www.ertms.net [retrieved: March, 2017].

[20] European Union, "Commission Decision of 25 January 2012 on the technical specification for interoperability relating to the control-command and signalling subsystems of the trans-European rail system," Official Journal of the European Union, vol. 55, pp. 1-51, February 2012.

[21] UNIFE, "A Unique Signalling System For Europe. The long journey to an interoperable railway system," Availale from htttp://www.ertms.net [retrieved: March, 2017].

[22] Ministry of Infrastructure and the Environment, "Derde Kadernota Railveiligheid," 2010 Available from: http://www.rijksoverheid.nl [retrieved: March, 2017].

[23] N.P. Hoj, and W. Kroger, "Risk analyses of transportation on road and railway from a European Perspective," Safety Science, vol. 40, pp. 337-357, 2002.

[24] J. Rasmussen, "Risk management in a dynamic society: a modelling problem," Safety Science, vol. 27, pp. 183-213, 1997.

[25] ERTMS Strategy Group, "National ERTMS Business Requirements," Available from: http://www.rssb.co.uk [retrieved: March, 2017].

[26] H. Priemus, "Mega-projects: Dealing with Pitfalls," European Planning studies, vol. 18, pp. 1023-1039, 2010.

[27] T. Pasquale, E. Rasaria, M. Pietro, and O. Antonio, "Hazard Analysis of Complex Distributed Railway Systems," Proceedings of the 22nd International Symposium on Reliable Distributed Systems (SRDS'03), October 2003, pp. 283-292, ISSN: 1060-9857, ISBN: 0-7695-1955-5.

[28] European Transport Safety Council (ETSC), "Transport accident and incident investigation in the European Union," Available from: http://www.etcs.eu [retrieved: March, 2017].

[29] European Railway Agency, "Analysis of Potential Interoperability Problems Final Report WP4," Available from: http://www.era.europea.eu [retrieved: March, 2017].

[30] European Railway Agency, "Subset-026—2 v300," Available from: http://www.era.europea.eu [retrieved: March, 2017].

[31] N. Leveson, "A new accident model for engineering safer systems," Safety Science, vol. 42, pp. 237-270, 2004.

[32] S. Dekker, "Drift into failure: from hunting broken components to understanding complex systems," CRC Press, 2011.

[33] G. Baxter, and I. Sommerville, "Socio-technical systems: From design methods to systems engineering," Interacting with Computers, vol. 23, pp. 4-17, January 2011.

[34] S. Nusser, "Robust Learning in Safety-Related Domains. Machine Learning Methods for Solving Safety-Related Application Problems," Doctoral Thesis, Univ., Fak. Für Informatik, 2009.

[35] B. Enserink, "Integral assessment – putting safety on the agenda for mitigation and preparedness," Safety Science, vol. 39, pp. 93-105, 2001.

[36] Tweede Kamer Der Staten-Generaal, "Verslagen van de openbare verhoren," Available from: http://www.tweedekamer.nl [retrieved: March, 2017].

[37] K. Schuitemaker, J.G. Braakhuis, and M. Rajabalinejad, "A Model Based Safety Architecture Framework for Dutch High Speed Train Lines," Proceedings of the 10th International Conference on System of Systems Engineering (SoSE), May 2015, pp. 21-29, 2015.

[38] Ministry of Infrastucture and the Environment, "Uitrolstrategie ERTMS," 2016 Availble from http://www.tweedekamer.nl [retrieved: March, 2017].

[39] The Duth Safety Board, "Train collision Amsterdam 2012 Westerpark," Available from: http://www.onderzoeksraad.nl [retrieved: March, 2017].

Supporting Risk-Based Design by Computational Synthesis

Mohammad Rajabalinejad, Robert Velten, Hans Tragter
Department of Design, Production and Management
Faculty of Engineering Technology, University of Twente, the Netherlands
Email: M.Rajabalinejad@utwente.nl, R.h.e.velten@student.utwente.nl, H.Tragter@utwente.nl

***Abstract*— Risk-based design often starts when the design details are available. Commonly used engineering tools focus on risk assessment for already-detailed designs. This study suggests using automated solutions for early design phases where efficient exploration of design space can lead to solutions that offer better performances with less risk. The paper states the problem, relevant works, and summarizes the steps taken in order to generate solutions for a product complicated to model. A real-world example application is presented.**

Keywords- risk-based design; automation; computational synthesis.

I. INTRODUCTION

Exploration of design space in early design phases is valuable for the project but is expensive. The importance of early design phases is discussed in different literatures [1, 2], yet there are other performance metrics forcing design engineers to assign a certain amount of resources to this phase.

The normal design phase starts with a concept which will be embodied and detailed later on. Since this process is time consuming and given the available resources, this often leads to limited choices for designers [3]. To overcome this limitation, the paper suggests using a detailed model in early design phases where automation provides many choices for the designer. From this palette of possibilities he or she can explore the design space easily and move toward the choices that are closer to the required performances and afford less risk.

A. Risk-based design

Risk is defined as multiplication of probability of failure and its consequence. In order to reduce risk, the probability of failure has to be small. Risk-based design is a promising approach for handling of complex problems [4, 5].

A simple search on google scholar for “risk-based design” finds more than 2800 articles or books. Yet risk based approach is not limited to design. There are literature works for example about risk-based reliability analysis, risk-based evaluation of design criteria, or risk-based decision making processes.

The deterministic approach in design does not fully match the expectations for reliability of products or systems and reveals shortcomings for future development. Limitations of deterministic approaches e.g. the use of safety factors have been discussed for example in [2]. In deterministic approach, safety factors are used to incorporate uncertainty, whereas risk-based design methodology uses probability distributions for risk estimation. The deterministic approach also requires a full scale prototype to be built and tested under working conditions. This, however, is not always a possibility.

In risk-based design process, the probability of failure is used to capture the uncertainties in the course of design process, often providing a more appropriate understanding of the problem. Furthermore, it can be utilized to make the design process more proactive and prepare for unexpected failures [2]. Risk-based design has been actively used in different industries producing standard methods for uncertainty measurement, risk assessment and management [6]. In many practices, however, this has been limited to realization of failure modes determined by designers or engineers. This is often possible only after having a detailed design which makes it costly and inefficient to come back and apply principal changes.

This research moves toward automation of risk-based design process. Integration of risk-based design with automation creates the advantages of both approaches resulting in more efficiency and robustness. And the results are promising, as discussed through the paper. Yet, to achieve its full potential, insight and experience involving the methodology need to be acquired. This has led to the following research question: ”What are the key performances to achieve for design of a specific product?”.

The methodology will be tested on a case by trying to find the best suited solution for this case. The automated part of the methodology uses a generic synthesis tool customised by the authors. The case needs to be translated into a model, which can be used in a computational design synthesis tool.

The remainder of the paper is structured as follows. Section II and III respectively explain the problem and method. Section IV presents an example application, and Section V concludes the paper.

II. PROBLEM STATEMENT

The lengthy process of early design makes the risk-based design a passive process that interferes less little with the early choices, when the designers have the most freedom to choose and change. Therefore, the problem is that treatment of risk during the last design phases causes designers to be reluctant to major changes. In this paper, we explore possible solutions to overcome this issue.

Copyright (c) IARIA, 2017. ISBN: 978-1-61208-549-4

III. THE METHOD

In order to design for risk effectively, one needs to bring the risk next to the other performance indicators considered by designers in early design. This will shorten the design process, and effectively make risk as one of the performance indicators through the design process.

IV. EXAMPLE APPLICATION

The example application presented here is an already existing pressure sensor produced by company STA (pseudo-name, the actual company name is not disclosed). The sensor works at a maximum diesel pressure of 400 MPa and measures the pressure of the injected fuel in an internal combustion engine (see Figure 1).

The sensor has screw-thread on the outside of the housing for screwing it in the common rail. Pressure of the diesel causes the topside to deform together with the attached strain gauges. The strain gauges provide the resulting information instantaneous to the engine's control unit (ECU). Not providing this information will lead to unforeseen and costly failures. Important part of the case will be the potential failure of the walls and the top of the topside of the sensor. When failing, diesel could start leaking and combust within the engine bay. This would result in even higher costs or even worse. For this part, risk-based design will be implemented.

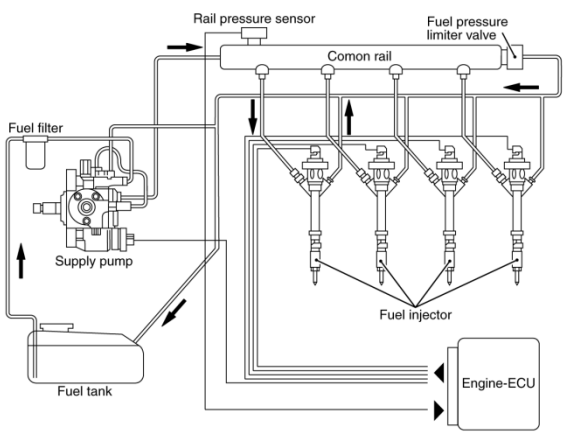

Figure 1. The pressure sensor placed within the system of the engine.

A. Downsized model

After considering the whole sensor, it became clear that all the electronic parts of the sensor could be discarded in the design process, as well as the bottom standardized part of the sensor. These parts where not important in the design process of the sensor, because these parts where similar for all types of sensors. This resulted in neglecting most of the parameters for the bottom of the sensor and leaving only the topside of the sensor (see Figure 2).

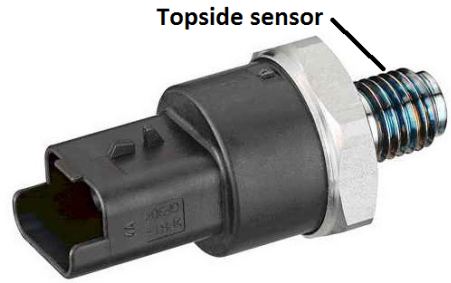

Figure 2. Top (half) of the sensor known as the total sensor

The topside of the sensor holds the key performances, risks and parameters to this design (see Figure 3). The optimal radius of the inside corners are already known at STA and thus will be used due to the fact that including them would overcomplicate the model (0.1 mm inside and 0.4 mm outside). For the same reason pre tensions from tightening the sensor will be excluded.

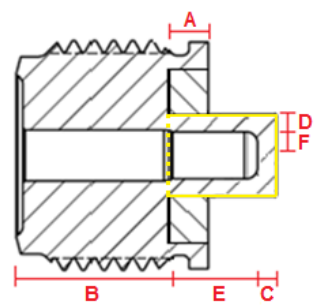

Figure 3. Cross section of the total sensor with the indicated parts (capital letters) for the equation of production cost

B. Model

The variable input parameters, which describe the simplified model (used for the sake of quick calculations), will be divided into dimensions and material parameters (see Table 1). Four ranges of different materials are used: Aluminium, 42CrMo4 steel, 17-4PH stainless steel and PTFE.

Having these parameters, one can calculate the weight, material price, inside volumes and production cost using the synthesis tool. Models have been constructed by the use of equations extracted from the disk and plate theory. For the ease of calculations, round disk/tube situations have been modeled to obtain the stress and deflection equations for the walls and topside. These models have been validated by a precise finite element model implemented in ANSYS software (www.ansys.com) given the accepted tolerance level of 10% (see Figure 4).

Copyright (c) IARIA, 2017. ISBN: 978-1-61208-549-4

TABLE 1. PARAMETERS OF THE DIMENSIONS AND MATERIALS

Dimensions	Parameter	in [mm]
Radius inside (F)	Rinside	[2, 4]
Length walls (E)	Lwalls	[3, 7]
Length bottom sensor (B)	Lbottom	[10, 20]
Length depth gap (A)	Lgap	[0, 3]
Thinkness walls (D)	Twalls	[1, 4]
Thinkness topside (C)	Ttopside	[0.5, 3]
Material parameters	**Name/unit**	
Name	String	
Young's modulus	E [Mpa]	
Poisson ratio	v [-]	
Density	Den [kg/mm³]	
Price	P [€/kg]	
StressMax	σmax [N/mm²]	

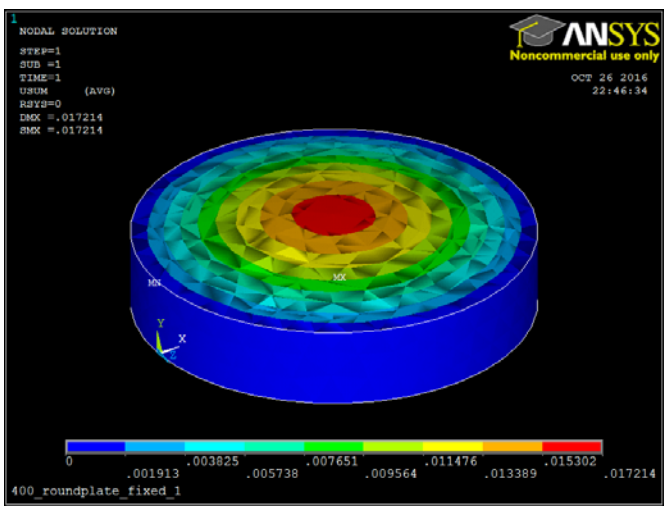

Figure 4. Deflection in the fixed round disk scenario (1,72e-2mm)

To verify the equations and have certain accuracy in the solutions, the equations had to be within a maximum range of 15% of the finite element model. It became clear that the round corners had a positive influence on the deflection on the topside. An adjustment had to be made combining the equation for a fixed round plate with 20% of the equation of a hinged round plate (read topside). All other equations were within their maximum scope.

C. *Results*

The model was implemented in the computational synthesis tool resulting in a set of possible solutions with their corresponding input parameters and performances. Two example set of solutions are given in Table 2.

TABLE 2. TWO SOLUTIONS OF THE MODEL (WITH THEIR INPUT PARAMETERS AND PERFORMANCES) GIVEN FOR TWO DIFFERENT MATERIALS

Input parameters [mm]	42CrMo4	17-4PH
Rinside	2,44	2,3
Lwalls	5,17	4,43
Lbottom	16,76	12,83
Lgap	0,76	2,75
Twalls	3,98	2,86
Ttopside	2,45	1,08
Performances		
Volume 1 [mm³]	96,7	73,7
Volume 2 [mm³]	409,8	287,3
Productioncost [$]	0,92	0,85
Weight [kg]	0,0102	0,0002
Price [€]	0,00023	0,00078
Deflection [mm]	0,0014	0,0129
Stress topside [N/mm²]	547,76	623,04
Stress walls [N/mm²]	263,29	1215,18

Both PTFE and Aluminium had no possible solution, within the range of input parameters, due to reaching the stress limit for these materials (as expected). To be able to find the most appropriate solutions a trade-off needs to be made between different performances and input parameters.

We observed that the importance of a clear understanding of the key performances is significant. It is important to notice that the approach does not necessarily lead to the optimum solution, yet it helps designers to compare different possible choices and make we-informed choices with regard to different parameters and performances.

The approach, therefore, supports designers to make better trade-offs by for example choosing the more appropriate material, thickness, etc..

V. CONCLUSIONS

Automation of risk based design process and exploration of different solutions in early design phases provide further insights for designers and helps choose more appropriate solutions with regards to risk.

To make well-informed choices and better trade-offs, a good understanding of key performance and key parameters is fundamental. In addition, a model with the right amount of information and detail is necessary. To properly utilize this process, a designer should be able to realize the key parameters and their relationship with the desire performance indicators e.g. risk.

REFERENCES

[1] G. Pahl, W. Beitz, J. Feldhusen, and K.-H. Grote, *Engineering Design A Systemmatic Approach*. Springer, 2007.

[2] B. S. Blanchard, W. J. Fabrycky, and W. J. Fabrycky, *Systems engineering and analysis*. Prentice Hall Englewood Cliffs, NJ, 1990.

[3] J. M. J. Becker, "From how much to how many, Managing Complexity in Routine Design Automation," PhD, Twente, 2010.

[4] J. Faulin, A. A. Juan, S. Martorell, and J.-E. Ramírez-Márquez, "Simulation Methods for Reliability and Availability of Complex Systems," (Reliability Engineering. 2010, p.^pp. Pages.

[5] M. Rajabalinejad, "Modelling and Prioritization of System Risks in Early Project Phases," *International Journal on Advances in Telecommunications,* vol. 9, no. 3-4, 2016.

[6] *BS EN 31010:2010 Risk management - Risk assessment techniques*, 2010.

Shift-Invariant Motif Discovery in Image Processing

Sahar Torkamani and Volker Lohweg, Senior Member, IEEE
inIT – Institute Industrial IT
Ostwestfalen-Lippe University of Applied Sciences
Lemgo, Germany
Email: {sahar.torkamani, volker.lohweg}@hs-owl.de

***Abstract*—Nowadays, the boost of optical imaging technologies results in more data with a faster rate are being collected. Consequently, data and knowledge discovery science has become an attractive and a fast growing topic in several industry and research area. Motif discovery in image processing aims to tackle the problem of deriving structures or detecting regularities in image databases. Most of the motif discovery methods first convert images into time series and then attempt to find motifs in such data. This might lead to information loss and also the problem of inability to detect shifted and multi-scale image motifs of different size. Here, a method is proposed to find image motifs of different size in image datasets by applying images in original dimension without converting them to time series. Images are inspected by the Complex Quad Tree Wavelet Packet transform which provides broad frequency analysis of an image in various scales. Next, features are extracted from the wavelet coefficients. Finally, image motifs are detected by measuring the similarity of the features. The performance of the proposed method is demonstrated on a dataset with images from diverse applications, such as hand gesture, text recognition, leaf and plant identification, etc.**

Keywords–Motif discovery; Image processing; Wavelet transformation.

I. Introduction

In this new millennium, the growth of digital computation and telecommunication has resulted in a flood of information. Most of this information is in the form of text, graphics, pictures, videos or integrated multimedia. In order to analyse and acquire efficient information from such datasets, data mining and machine learning tasks are essential. These tasks can be categorized into clustering, classification, anomaly detection and *motif discovery*.

In order to perform the aforementioned tasks, one needs to have information such as number of clusters or classes, prototype patterns/images for each class and a given image query to find [1]. The problems of clustering or classifying images as well as finding the query images in an image database have been investigated during last decades [2]–[4]. However, the problem of deriving structures or detecting regularities in image databases is rather new topic and investigated by researchers [5]. Detecting frequently repeated unknown images in a data base without any prior information is called motif discovery. The term motif finds its origin in genetics and Deoxyribonucleic Acid (DNA) sequence. A sequence motif in a DNA is a widespread amino-acid sequence pattern which shows a biological significance [6]. However, this term was first triggered by Patel et al. [7] in time series data mining.

Motifs provide valuable insights about the investigated problem to the user. In the past decade, huge research effort has been performed on this topic [5] [8]. However, most of the image motif discovery methods, first convert images into one-dimensional time series and then attempt to find motifs in such data. This might leads to information loss and also the problem of inability to detect shifted and multi-scale motifs of different size [9]. Correspondingly, a method is proposed to find shifted and multi-scale motifs of different size in image datasets by applying the images in original dimension without converting them to one dimensional time series.

The paper is structured as follows: the related work in motif discovery for image data type is described in Section II. The proposed approach is explained in Section III. Next, evaluation of this method and the obtained results are illustrated in Section IV. Finally, the directions of the future work and a conclusion are indicated in Section V.

II. Related Work

Image and shape analysis have been a matter for discussion over the past decades. Huge amount of research has been performed in several image processing tasks such as clustering, classification, query by content, segmentation, etc. [3], [10]–[13]. Recently, motif discovery in image and shape analysis has gained great interest. Researchers aimed to link time series data mining tasks and issues to the image and shape analysis domain [5] [9] [14].

First, Xi et al. [9] tried to detect image motifs in image data sets. Nevertheless, their approach is based on representing an image or a shape in a one dimensional time series. The main problem of such an approach is that transforming a two dimensional data to a one dimensional might lead to information loss.

Chi et al. [15] applied the same procedure as in [9] in order to detect image motifs in face image data sets. Ye and Keogh [14], as well as Grabocka et al. [16] extended the proposed approach in [9] by introducing the term shaplet. After transforming an image to a one dimensional representation, instead of analysing the whole time series only a discriminative subsequence of the time series will be considered. Although the performance of these methods is promising, but these approaches transform the data to a one dimensional time series.

Recently, Rakthanmanon and his colleagues [17] aimed to tackle this problem by detecting motifs in image data without representing them into a one dimensional signal. In [17], first images are segmented using a sliding window of a fixed size, then the similarity between these segments are measured by the generalized Hough transform. One of the drawback of this method is the size of the window. This results in inability of detecting motifs with various proportions. En et al.

Copyright (c) IARIA, 2017. ISBN: 978-1-61208-549-4

[18] followed a similar approach, nevertheless they employed sliding windows with varying sizes of 20, 40, 80, 160 pixels.

In our previous approach [19] motifs in an image data base are discovered in their original dimension without converting them to time series. Images are decomposed into several frequency scales by the dual tree complex wavelet transform (DTCWT) [20], next features are extracted from the wavelet coefficients and finally motif images are found by measuring the similarity of their features. However, further experiments showed that the DTCWT is shift tolerance and not shift invariant [21]. For this reason, in this work, an approach is proposed which is based on a shift-invariant feature extraction method for motif discovery (SIMD), given in [21]. This method is applied as core in our approach and explained in the following section.

III. Proposed Approach

The sketch of our approach is depicted in Figure 1.

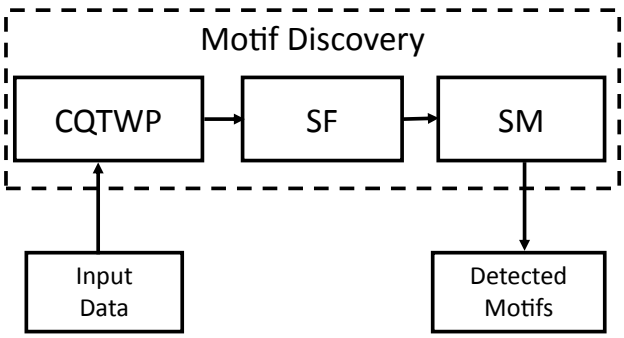

Figure 1. The proposed approach; CQTWP is the Complex Quad Tree Wavelet Packet; SF are the statistical features and SM are similarity measures.

In the first step, images are transformed by the *Complex Quad Tree Wavelet Packet* (CQTWP) into a broad frequency scales. After that features are extracted from the normalized wavelet coefficients. Finally, motifs are discovered by measuring the similarity between features using various distance measures. These steps are explained in details in the following.

A. Complex Quad Tree Wavelet Packet Transform

1) 1D-CQTWP: The CQTWP is an extended version of the DTCWT [20] and it consists of two wavelet packet trees working parallel to each other; namely "WPT A" and "WPT B" where "WPT A" represents the real part and "WPT B" provides the imaginary part of the signal. Figure 2 is a graphical representation of the "*1D-WPT A*", where $\downarrow 2^e$ and $\downarrow 2^o$ depict the even and odd down-sampling.

The wavelet and scaling functions of the CQTWP are defined as:

Definition 1. *Let* $\psi_{a,2J+1}(t)$,$\psi_{a,2J+3}(t)$, $\psi_{b,2J+1}(t)$, $\psi_{b,2J+3}(t)$ *and* $\phi_{a,2J}(t)$,$\phi_{a,2J+2}(t)$, $\phi_{b,2J}(t)$, $\phi_{b,2J+2}(t)$ *be the wavelet and scaling functions of the CQTWP. For convenience both wavelet transforms are considered as orthonormal. The wavelet and scaling functions in "WPT A",*

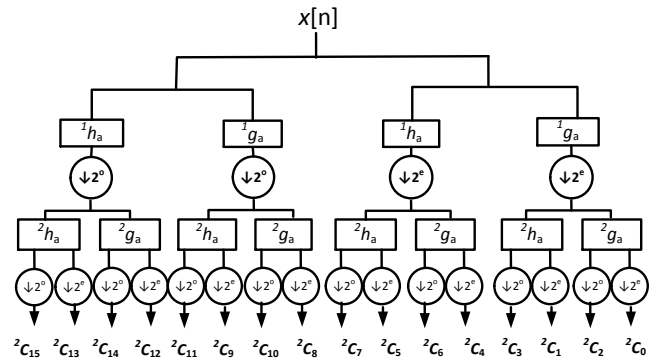

Figure 2. First wavelet packet filter bank of a two scale CQTWP. The filters ${}^s g_a$ and ${}^s h_a$ are low and high pass filters and s is the number of scales.

$\forall n \in \mathbb{N}$ *are given by*

$$
\begin{aligned}
{}^{s+1}\psi_{a,2J+1}(t) &= \sqrt{2}\sum_{n=0}^{M} {}^s h_a[n]\ {}^s\phi_{a,2J}(2t-n),\\
{}^{s+1}\psi_{a,2J+3}(t) &= \sqrt{2}\sum_{n=0}^{M} {}^s h_a[n]\ {}^s\phi_{a,2J+2}(2t-n+1),\\
{}^{s+1}\phi_{a,2J}(t) &= \sqrt{2}\sum_{n=0}^{M} {}^s g_a[n]\ {}^s\phi_{a,2J}(2t-n),\\
{}^{s+1}\phi_{a,2J+2}(t) &= \sqrt{2}\sum_{n=0}^{M} {}^s g_a[n]\ {}^s\phi_{a,2J+2}(2t-n+1).
\end{aligned}
$$

Parameter $J = 2j$ *where* $0 \le j < 2^s \cdot (s-1)$, *and* $s \in \mathbb{N}$ *is number of scales.*

For "WPT B" the wavelet and scaling functions are defined in the same manner, but the high-pass filter ${}^s h_a$ *and the low-pass filter* ${}^s g_a$ *are replaced by* ${}^s h_b$ *and* ${}^s g_b$ *respectively. All filters are causal so* ${}^s h_{a,b}[n] = 0$ *and* ${}^s g_{b,b}[n] = 0$ *for* $n < 0$.

The CQTWP applies the same filters as the DTCWT whereby the filters are real and orthonormal. In the first scale, the filters have the even-length of 10 [22] and in the scale greater than one, filters have the even-length of 14. Both filters form a Hilbert pair due to their design [20].

Definition 2. *Wavelets* ψ_a *and* ψ_b *with the following property*

$$
\Psi_a(j\omega) = \begin{cases} -j\Psi_b(j\omega), & \omega > 0,\\ j\Psi_b(j\omega), & \omega < 0,\end{cases}
$$

are called the Hilbert pair, *where* $\Psi(j\omega)$ *is the Fourier transform of* $\psi(t)$.

This means, the response of each branch of the "WPT A" and the corresponding branch of the "WPT B" forms a Hilbert pair. Consequently, the CQTWP is approximately analytic in each sub band. The analytic representation has advantages such as reduction of aliasing.

The CQTWP has another advantage of being shift-invariant [21]. This property is achieved by decomposing a non shifted and a shifted version of the input signal in each scale. Shift-invariance property results in identical wavelet coefficients for

both the original signal and its shifted versions. In other words, the wavelet and scaling functions of the CQTWP select both even and odd samples of the signal in order to detect the occurred shift. For simplicity, the wavelet and scaling functions of "WPT A" are denoted by $\psi_{a,e}(t) = \psi_{a,2J+1}(t)$ and $\psi_{a,o} = \psi_{a,2J+3}(t)$; and $\phi_{a,e} = \phi_{a,2J}(t)$, $\phi_{a,o} = \phi_{a,2J+2}(t)$. The functions of "WPT B" are represented in the same manner. The proof of shift invariance property of the CQTWP is given in [21].

2) 2D-CQTWP: The first scale of the 2D-CQTWP is similar to the 2D-discrete wavelet transform [23], where an image is decomposed into four sub bands namely LL_1, LH_1, HL_1 and HH_1, cf. Figure 3(a). However, in the first scale the 2D-CQTWP has two LL, two LH, two HL and two HH sub bands obtained from both "*2D-WPT A*" and "*2D-WPT B*".

The structure of two scales decomposition of the "*2D-WPT A*" is depicted in Figure 3(b) where both low and high-pass filtered sub bands decomposed further. This property results in a more flexible and broad frequency decomposition of the images.

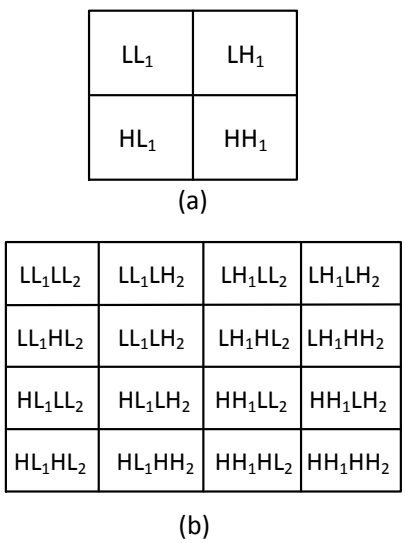

Figure 3. Structure of two scales decomposition of the "*2D-WPT A*": (a) the first scale decomposition, (b) the second scale decomposition.

LL_1 is the product of the low-pass function $\phi_a()$ along the first dimension (row) and the low-pass function $\phi_a()$ along the second dimension (column). LH_1 is the product of the low-pass function $\phi_a()$ along the first dimension (row) and the high-pass function $\psi_a()$ along the second dimension (column). Similarly the HL_1 and HH_1 are labelled, and the index 1 determines the decomposed scale. The same procedure is performed on each subband in order to obtain the second scale coefficients.

The wavelet and scaling functions of the 2D-CQTWP are defined as:

Definition 3. *The "2D-WPT A"of the 2D-CQTWP is characterized by twelve wavelets and four scaling functions. The 2D-wavelet $\psi(x,y) = \psi(x)\psi(y)$ is associated with the row-column implementation of the wavelet transform. The wavelet functions for the wavelet packet tree A are given by*

$$\psi_{a,1}(x,y) = \phi_{a,e}(x)\psi_{a,e}(y), \qquad \psi_{a,4}(x,y) = \phi_{a,e}(x)\psi_{a,o}(y),$$

$$\psi_{a,2}(x,y) = \psi_{a,e}(x)\phi_{a,e}(y), \qquad \psi_{a,5}(x,y) = \psi_{a,e}(x)\phi_{a,o}(y),$$

$$\psi_{a,3}(x,y) = \psi_{a,e}(x)\psi_{a,e}(y), \qquad \psi_{a,6}(x,y) = \psi_{a,e}(x)\psi_{a,o}(y).$$

The rest of the wavelet functions are obtained similarly. The scaling functions are defined as

$$\phi_{a,1}(x,y) = \phi_{a,e}(x)\phi_{a,e}(y), \qquad \phi_{a,2}(x,y) = \phi_{a,e}(x)\phi_{a,o}(y),$$

$$\phi_{a,3}(x,y) = \phi_{a,o}(x)\phi_{a,e}(y), \qquad \phi_{a,4}(x,y) = \phi_{a,o}(x)\phi_{a,o}(y).$$

The wavelet and scaling functions of the "2D-WPT B" are given accordingly.

B. Feature Extraction

Features present the special characters of the data, therefore it is important that they are detectable under changes in proportion, location or even under noise circumstances. Before extracting features, coefficients of each scale must be normalized by a normalized histogram. The normalized histogram $H(p)$ is given by

$$H(p) = \frac{1}{v \cdot u} \cdot h(p),$$

where $u, v \in \mathbb{N}$ determine the size of the matrix coefficients and parameter p is number of the histogram bins. The rate in each bin is presented by $h(p)$.

The extracted features are the first four statistical moments [24], namely, mean value, variance, skewness and kurtosis which are derived from the wavelet coefficients in both wavelet packet trees. As CQTWP is shift-invariant, then these features have identical values even in the case of shift occurrence in the data.

The scaling and wavelet functions of the CQTWP are orthonormal, and according to the Parseval's theorem the energy of the signal (image) is preserved in the coefficients. Therefore, the energy of the wavelet coefficients and their shifted ones are similar. As a result, in addition to statistical features, energy of the wavelet coefficients is considered as another feature.

C. Similarity Measures

In order to detect image motifs, the similarity between their features must be measured. Most cited and applied distance similarity measures in motif discovery are: two members of the Minkowski distance family [25], and Dynamic Time Warping (DTW) [25], which are applied as well in this work. The two members of the Minkowski distance or L_p-distance, Euclidean distance (ED) and Canberra distance (CD), both have linear computational time complexity $O(n)$, and are metric.

The Euclidean distance is obtained by setting $p = 2$ in L_p-distance. This measure is also known as L_2-distance. Besides the advantages of the Euclidean distance, results of this similarity measure are not promising in the case of outliers. The Canberra distance is actually a weighted version of Manhattan distance or L_1-distance, and is useful in the case of ranking lists or results.

DTW matches various sections of a time series by warping of the time axis, or finding the proper alignment. This similarity measure is more flexible than Euclidean or Canberra distance although its time-complexity is $O(n^2)$. Besides its quadratic computational time complexity, still DTW is one of the most popular approaches for measuring similarity/dissimilarity.

IV. Experiments and Results

To evaluate the performance of the proposed approach, the results are analysed by different quality measures, explained in the following. Next, the captured results of image motif discovery are presented.

A. Quality Measures

A perfect image motif is the one which matches all the images in the target class and no other images out of that class. To evaluate the result following quality measures are employed [1]: Correct motif discovery rate CR, Sensitivity Sn, Precision Pr and F-Measure $F-M$. These quality measures are based on four possibilities to qualify a motif matching an image; namely, true positive rate (TP), false negative rate (FN), true negative rate (TN), and false positive rate (FP).

Correct motif discovery rate is given by $CR = \frac{n^+}{N}$ where N is number of all motifs and n^+ is number of correctly detected motifs. Sensitivity ($Sn = \frac{TP}{TP+FN}$) measures the capacity of images of the target class correctly matched by the motif, Precision ($Pr = \frac{TP}{TP+FP}$) provides the fraction of images of the target class that are matched by the motif and the images that are not correctly matched by the motif and finally both precision and sensitivity are considered by F-Measure ($F-M = 2 \cdot (\frac{Pr \cdot Sn}{Pr+Sn})$) [1].

B. Results and Evaluation

The test image data base consists of images from diverse applications and domains like hand gesture and leaf identification [26], [27]. All the tests are executed with a 3.40 GHz Intel(R) core processor with 8GB RAM. The codes are performed by MATLAB R2015b [28]. In Figure 4, images of four groups are depicted. These images have various size and scale, since the proposed method is able to handle both images of fixed and variable size.

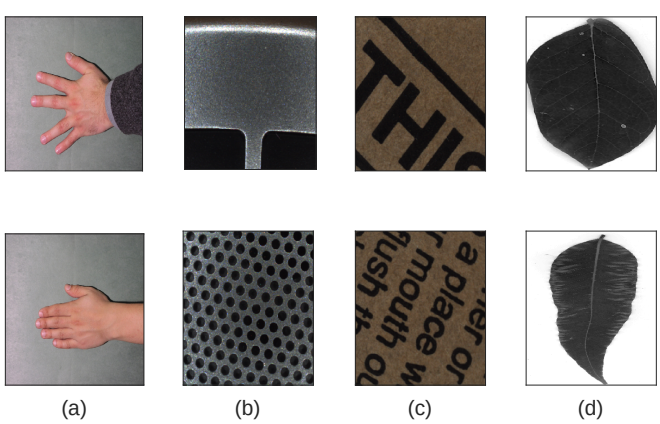

Figure 4. Data set of different images.

Among these images, the pictures of hands and leaves are the most occurred images (top inserted image motifs). Figure 5 shows the inserted image motifs (hand and leaf). In order to demonstrate the shift-invariant property of the 2D-CQTWP in feature space, images (b-d) are considered. These images are the shifted version of the image (a), and image (e) is the rotated version of image (a). Images (f-j) are different leaf types.

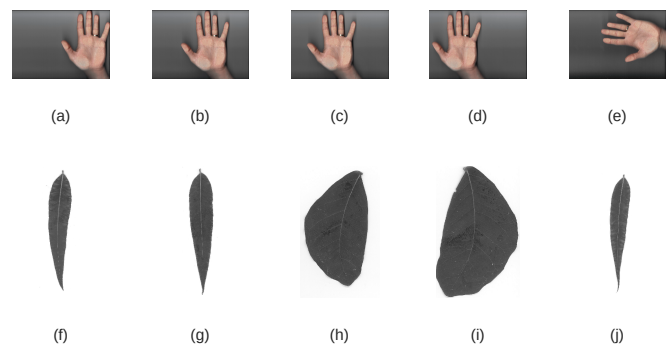

Figure 5. Images of hands and leaves. Images (b-d) are the shifted version of image (a); Image (e) is the rotated version of image (a). Images (f-j) are various sorts of leaves.

In the preprocessing step, all the images are presented in grey-scale, since the colour information is not required. Next, all the images are sent to 2D-CQTWP and decomposed into various scales. In this work, the wavelet coefficients of the second scale are selected, since the amount of noise is usually reduced in the second scale for the noisy data. The normalized histogram of the wavelet coefficients are calculated. Figure 6 is the graphical representation of the normalized histogram of the HL sub band coefficients of "2D-WPT A".

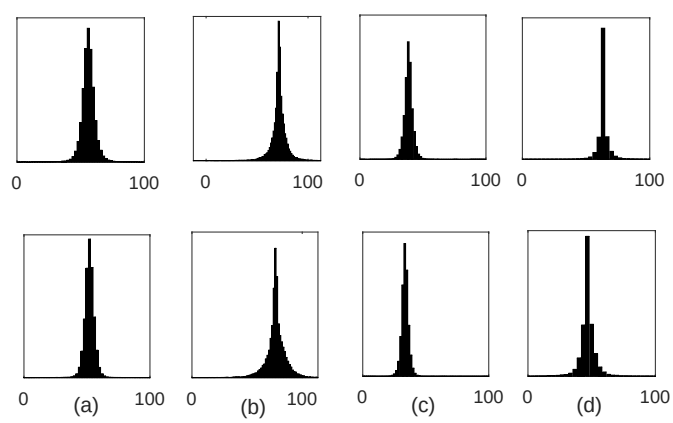

Figure 6. Normalized histogram of the HL sub band coefficients, obtained from the corresponding images from Figure 4 (a-d).

As depicted, the histograms of wavelet coefficients from the two depicted images in each group (a), (b), (c) and (d) are similar to each other but different to the histograms of other groups. This helps to determine the variations between various motif classes (inter-class).

The shift-invariant property of the 2D-CQTWP can be observed in Figure 7. A hand pattern and its shifted version is depicted in Figure 7 (a)-(b), where the position of the hand is changed. The normalized histogram of the HL sub band coefficients are given in Figure 7 (c)-(d) respectively. Since the 2D-CQTWP is shift-invariant, the histograms are identical to each other.

Next, the five stated features are extracted from the histograms of the wavelet coefficients in each scale. The efficiency of these features are tested by the linear discriminant

Copyright (c) IARIA, 2017. ISBN: 978-1-61208-549-4

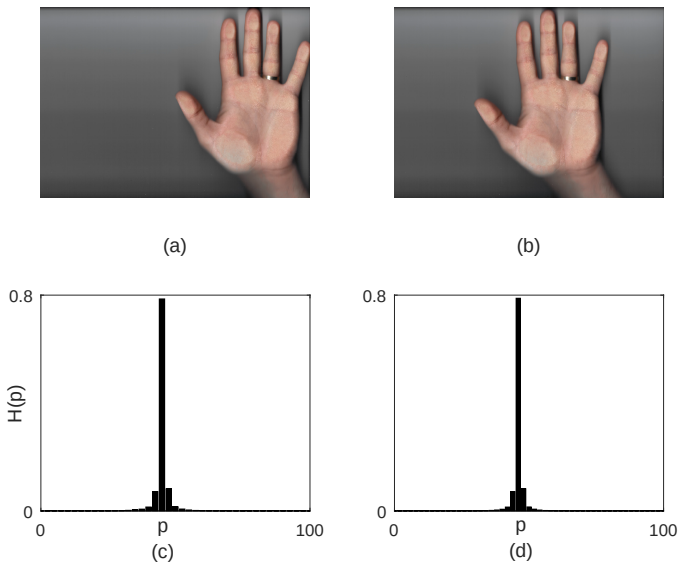

Figure 7. (a) a hand pattern; (b) shifted version of image in (a); (c) and (d) represent the normalized histograms of the HL sub band coefficients from images (a) and (b).

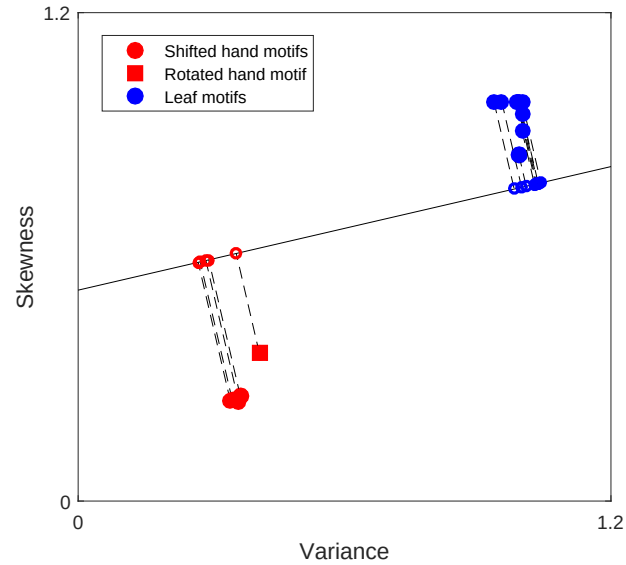

Figure 8. LDA projection of the two features from the hand and leaf image motifs; the distance between features within an image motif group is as minimum as possible and the distance between features of different image motif groups is large enough.

analysis (LDA) algorithm [1] [29].

LDA is a supervised method which projects the features from the samples of the two or more classes onto a lower dimensional space with good class separability in order to avoid over-fitting and computational costs reduction. This method provides a combination of features which separates the classes ideally with the minimum amount of error. The less the minimum error, the better is merit of the features. If the data can be separated linearly and correctly the error will be 0, and if the whole data cannot be classified linearly and correctly then the error has its maximum amount of 1. LDA finds the most discriminant projection by maximizing between-class distance and minimizing within-class distance. The experiments show that for most of the tested features the minimum error is between 0 and 0.01. Furthermore, the distance between feature clusters should be as great as possible to facilitate grouping.

Figure 8 demonstrates the result of the LDA projection of the two extracted features from the image motifs in Figure 5. It is obvious that the distance between the two groups is large enough in order to separate them correctly. Moreover, the distance between features belonging to the same image motif group (represented on the projection line) is minimized.

Since the 2D-CQTWP is shift-invariant, the first four hand images are as close as possible to each other and their projection on the projection line is at the same position. These images are depicted by the circle red marker. Nevertheless, the projection of the features extracted from the rotated image (illustrated by the square red marker) is not at the same position of other hand images. This illustrates that the 2D-CQTWP is not rotation invariant, however we are able to detect this image motif and separate it from other image motifs.

In the last step, the similarity between feature values is measured by Euclidean, Canberra and Dynamic Time Warping distance measures. Both Euclidean distance and Dynamic Time Warping performed similar in the case of small datasets (less than 50 images). These measures were able to detect 22 image motifs out of 25 inserted image motifs. The Canberra distance was able to discover 21 image motifs in the same data base.

Results of the stated similarity measures in Section III-C are depicted in Table. I. The presented results are obtained from the tested data set with 50 different inserted image motifs. Both Euclidean and DTW distance outperformed the Canberra distance. Euclidean and DTW distances detected the same amount of image motifs but, the image motifs were different. Since, the aforementioned image motif discovery approaches in Section II convert an image in a one dimensional signal, it is not possible to benchmark the performance of the proposed method against them.

TABLE I. Evaluating results of detected motifs, CR: Correct motif discovery rate, F-M: F-Measure, Sn: Sensitivity, Pr: Precision; ED: Euclidean distance, DTW: Dynamic Time Warping and CD: Canberra distance.

Similarity Measure	CR(%)	F-M(%)	Sn(%)	Pr(%)
ED	84.62	84.94	85.27	84.62
DTW	84.62	84.94	85.27	84.62
CD	83.85	84.82	85.83	83.85

V. Conclusion and Outlook

In this contribution, a method is presented to detect image motifs of various size. Detection of image motifs is performed within three steps: First, the Complex Quad Tree Wavelet Packet transform is applied to provide a comprehensive analysis of images in various frequency scales. This wavelet transform has efficient properties such as being shift-invariant. Moreover, its ability for analytic representation, is helpful in order to reduce aliasing.

The first four statistical moments and energy of the wavelet coefficients are extracted as feature values. Since motif discovery is an unsupervised task, there is no information about the tested images. Consequently, the statistical features are applied in this work, but depending on the task it is possible to employ other types of features.

In the next step, motifs are detected by measuring the similarity between their feature values. The performance of the proposed method is evaluated by different quality measures. One advantage of the proposed method is its ability to consider both images of fixed and variable lengths. In addition, as images are not transformed to a one dimensional representation form, no information is lost.

In the next approach, our aim will be to find the proper scale and nodes of the 2D-CQTWP with the best information content. Moreover, it is desirable to detect motifs within various images without segmenting them via a sliding window.

ACKNOWLEDGMENT

This research is partly supported by the International Graduate School of Intelligent Systems in Automation Technology (ISA), which is run by scientists of the Faculty of Computer Science, Electrical Engineering and Mathematics and the Faculty of Mechanical Engineering of the University of Paderborn and the Institute of Industrial Information Technologies (inIT) of the Ostwestfalen-Lippe University of Applied Sciences.

REFERENCES

[1] E. Alpaydın, Introduction to Machine Learning, 2nd ed. Cambridge: The MIT Press, 2010.

[2] S. A. Khan, M. Nazir, S. Akram, and N. Riaz, "Gender classification using image processing techniques: A survey," in 2011 IEEE 14th International Multitopic Conference. IEEE, 2011, pp. 25–30.

[3] S. S. Nath, G. Mishra, J. Kar, S. Chakraborty, and N. Dey, "A survey of image classification methods and techniques," in International Conference on Control, Instrumentation, Communication and Computational Technologies (ICCICCT). IEEE, 2014, pp. 554–557.

[4] S. Gangwar and R. P. Chauhan, "Survey of clustering techniques enhancing image segmentation process," in 2015 Second International Conference on Advances in Computing and Communication Engineering. IEEE, 2015, pp. 34–39.

[5] P. Esling and C. Agon, "Time-series data mining," vol. 45. ACM, 2012, pp. 1–34.

[6] M. K. Das and H.-K. Dai, "A survey of dna motif finding algorithms," BMC bioinformatics, vol. 8 Suppl 7, 2007, p. S21.

[7] P. Patel, E. Keogh, J. Lin, and S. Lonardi, "Mining motifs in massive time series databases," in Proceedings IEEE International Conference on Data Mining. IEEE, 2002, pp. 370–377.

[8] S. Torkamani and V. Lohweg, "Survey on time series motif discovery," in Journal: Wiley Interdisciplinary Reviews: Data Mining and Knowledge Discovery. Article ID: WIDM1199, 2017.

[9] X. Xi, E. Keogh, L. Wei, and A. Mafra-Neto, "Finding motifs in a database of shapes," in Proceedings of the 2007 SIAM international conference on data mining. SIAM, 2007, pp. 249–260.

[10] W. Hu, R. Hu, N. Xie, H. Ling, and S. Maybank, "Image classification using multiscale information fusion based on saliency driven nonlinear diffusion filtering," IEEE Transactions on Image Processing, vol. 23, no. 4, 2014, pp. 1513–1526.

[11] N. M. Zaitoun and M. J. Aqel, "Survey on image segmentation techniques," Procedia Computer Science, vol. 65, 2015, pp. 797–806, elsevier.

[12] K. Zhang, W. K. Leow, and Y. Cheng, Performance Analysis of Active Shape Reconstruction of Fractured, Incomplete Skulls. Springer International Publishing, 2015, pp. 312–324.

[13] B. K. Gayathri and P. Raajan, "A survey of breast cancer detection based on image segmentation techniques," in 2016 International Conference on Computing Technologies and Intelligent Data Engineering (ICCTIDE'16). IEEE, 2016, pp. 1–5.

[14] L. Ye and E. Keogh, "Time series shapelets: A new primitive for data mining," in Proceedings of the 15th ACM SIGKDD International Conference on Knowledge Discovery and Data Mining, ser. KDD '09. ACM, 2009, pp. 947–956.

[15] L. Chi, Y. Feng, H. Chi, and Y. Huang, "Face image recognition based on time series motif discovery," in IEEE International Conference on Granular Computing. IEEE, 2012, pp. 72–77.

[16] J. Grabocka, N. Schilling, M. Wistuba, and L. Schmidt-Thieme, "Learning time-series shapelets," in Proceedings of the 20th ACM SIGKDD International Conference on Knowledge Discovery and Data Mining, ser. KDD '14. ACM, 2014, pp. 392–401.

[17] T. Rakthanmanon, Q. Zhu, and E. Keogh, "Mining historical documents for near-duplicate figures," in IEEE 11th International Conference on Data Mining. IEEE, 2011, pp. 557–566.

[18] S. En, C. Petitjean, S. Nicolas, and L. Heutte, "Segmentation-free pattern spotting in historical document images," in 13th International Conference on Document Analysis and Recognition (ICDAR). IEEE, 2015, pp. 606–610.

[19] S. Torkamani, H. Dörksen, and V. Lohweg, "Multi-scale motif discovery in image processing," in Workshop on Probabilistic Graphical Models, Heidelberg, Germany, Oct 2015.

[20] I. W. Selesnick, R. G. Baraniuk, and N. G. Kingsbury, "The dual-tree complex wavelet transform," Signal Processing Magazine, IEEE, vol. 22, no. 6, 2005, pp. 123–151.

[21] S. Torkamani and V. Lohweg, "Shift-invariant feature extraction for time-series motif discovery," in 25. Workshop Computational Intelligence, ser. Schriftenreihe des Instituts für Angewandte Informatik - Automatisierungstechnik am Karlsruher Institut für Technologie, vol. 54. KIT Scientific Publishing, 2015, pp. 23–45.

[22] A. F. Abdelnour and I. W. Selesnick, "Symmetric nearly shift-invariant tight frame wavelets," IEEE Transactions on Signal Processing, vol. 53, no. 1, 2005, pp. 231–239, IEEE.

[23] C. S. Burrus, R. A. Gopinath, and H. Guo, Introduction to wavelets and wavelet transforms: A primer. Upper Saddle River and NJ: Prentice Hall, 1998.

[24] A. D. Polyanin and A. V. Manzhirov, Handbook of mathematics for engineers and sciencists. Boca Raton: Chapman & Hall/CRC, 2007.

[25] M. M. Deza and E. Deza, Encyclopedia of distances. Springer, 2009.

[26] M. B. Stegmann and D. D. Gomez, "A brief introduction to statistical shape analysis," 2002, informatics and Mathematical Modelling, Technical University of Denmark, DTU.

[27] P. F. B. Silva, A. R. S. Marcal, and da Silva R. A., "UCI machine learning repository: Leaf data set," 2014, last access: 06.04.17. [Online]. Available: https://archive.ics.uci.edu/ml/datasets/Leaf

[28] MathWorks, "MATLAB," 2017, last access: 06.04.17. [Online]. Available: https://de.mathworks.com/products/matlab.html

[29] C. Bayer, M. Bator, U. Mönks, A. Dicks, O. Enge-Rosenblatt, and V. Lohweg, "Sensorless drive diagnosis using automated feature extraction, significance ranking and reduction," in 18th IEEE Int. Conf. on Emerging Technologies and Factory Automation (ETFA 2013). IEEE, 2013, pp. 1–4.

A Survey on CNN and RNN Implementations

Javier Hoffmann, Osvaldo Navarro, Florian Kästner, Benedikt Janßen, Michael Hübner
Chair for Embedded Systems of Information Technology
Ruhr-Universität Bochum
Bochum, Germany
Email: {Javier.Hoffmann;Osvaldo.NavarroGuzman;Florian.Kaestner;Benedikt.Janssen;Michael.Huebner}@rub.de

***Abstract*—Deep Neural Networks (DNNs) are widely used for complex applications, such as image and voice processing. Two varieties of DNNs, namely Convolutional Neuronal Networks (CNNs) and Recurrent Neuronal Networks (RNNs), are particularly popular regarding recent success for industrial applications. While CNNs are typically used for computer vision applications like object recognition, RNNs are well suited for time variant problems due to their recursive structure. Even though CNNs and RNNs belong to the family of DNNs, their implementation shows substantial differences. Besides more common Central Processing Unit (CPU) and Graphic processing Unit (GPU) implementations, Field Programmable Gate Array (FPGA) implementations offer great potential. Recent evaluations have shown significant benefits of FPGA implementations of DNNs over CPUs and GPUs. In this paper, we compare current FPGA implementations of CNNs and RNNs and analyze their optimizations. With this, we provide insights regarding the specific benefits and drawbacks of recent FPGA implementations of DNNs.**

Keywords–deep learning, convolutional, recurrent, neural network.

I. Introduction

Deep learning is a powerful method for supervised learning without the need of feature engineering. The resulting Deep Neural Networks (DNN) can represent functions of high complexity due to the size of the network depending on the number of hidden layers and neurons or units inside each layer [1]. Two varieties of DNNs, Convolutional Neural Networks (CNNs) and Recursive Neural Networks (RNNs), have especially shown great potential to real-life applications. While CNNs are typically used for imagery classification [2][3], RNNs are suitable for time-variant problems like speech recognition [4] due to their recursive structure.

A. Convolutional Neural Networks

CNNs are a type of feed-forward artificial neural network [1]. Figure 1 shows a diagram of a simple CNN. CNNs usually consists of the following components: convolution, evaluation of a non-linear activation function, pooling or sub sampling and classification or regression. The convolution component extracts features from the input image with a set of learnable filters or kernels called feature maps. The convolution computation is done through a dot product between the entries of the kernel and the input section of same size across the entire input frame. The output of the dot-product is forwarded to an activation function, typically $sigmoid()$, $ReLU()$ or $tanh()$, which increases the nonlinear properties of the CNN. Then, the pooling component reduces the dimensionality of each feature map and keeps the most important information for the classification component. In modern CNNs, like ImageNet [5], these three stages alternate several times. At the next stage of the feed-forward path, one or more fully-connected layers are applied to extract the classification or regression information with the help of logistic or linear regression. The training of CNNs is done via gradient-based backpropagation algorithm.

B. Recurrent Neural Networks

RNNs extend the concept of conventional feed-forward neural networks by having a hidden recurrent state. The activation of the hidden recurrent state depends on the previous activations [6]. Thus, unlike conventional neuronal networks, they can include timing information in the processing, which is important for instance for speech recognition [7].

One of the first approaches in the direction of today's RNNs was done by Jain et al. They developed a partially RNN to learn character strings [8]. The feedback connection enables RNNs to represent previous inputs as activation [9]. According to Jain et al. [8] the architecture of RNN can be anything between a fully interconnected network and a partially interconnected network. In fully interconnected networks, every neuron is connected to every other neuron, as well as itself via feedback connections, allowing to transfer states during-run time. This is depicted in Fig. 2, where the unfolded structure at the bottom shows the behavior of a self-feedback connection. However, in contrast to Fig. 2, for a fully interconnected RNN, there are no distinct input and output layers.

In the 90s, there have been difficulties to train RNNs for applications, whose data includes dependencies over long temporal intervals. The first contribution to a network to overcome the issue of learning long-term dependencies was made by Hochreiter and Schmidhuber [9]. They proposed a new recurrent network architecture, together with a gradient-based learning algorithm, called Long Short-Term Memory networks (LSTM). These networks can be categorized as a sub-group of RNNs. The network architecture LSTM cells is depicted in Fig. 3.

C. CNN and RNN Implementations

There have been several approaches to accelerate the training and the feed-forward path of CNNs and RNNs. Within the scope of this paper, we focus on the forward-path implementation on different platforms: Aplication Specific Integrated (ASIC),Fiel Programmable Gate Array (FPGA) and Graphic Processing Unit (GPU). These platforms distinguish in terms of performance, flexibility and energy consumption.

The use of CNNs and GPUs as accelerators has turn common, achieving significant speedups and better scalability in comparison with a general-purpose processor [10]. The possibility to train DNNs with the help of GPUs is one of the main reasons of their recent success, due to the high-performance speedup caused by the utilization of massive

Copyright (c) IARIA, 2017. ISBN: 978-1-61208-549-4

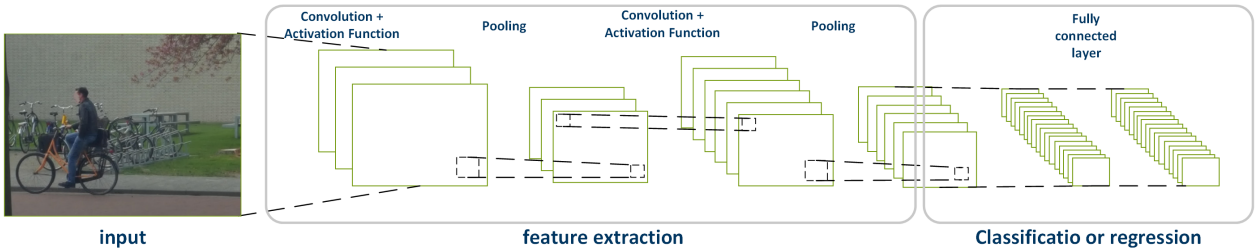

Figure 1. Common processing flow of a convolutional neural network [1].

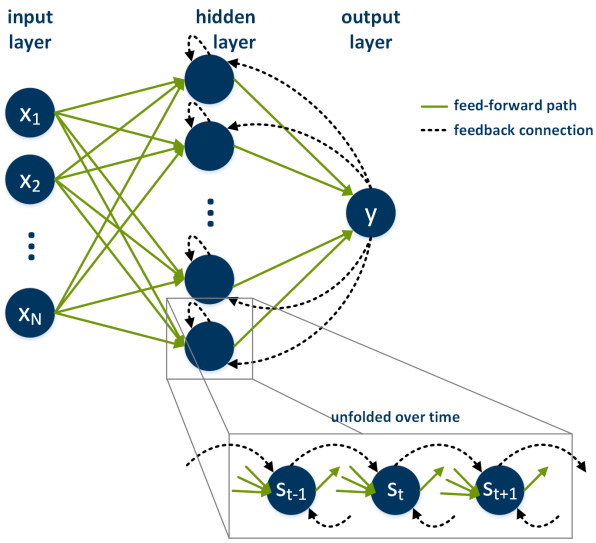

Figure 2. Principle of RNNs, layers are connected to their predecessors via feedback connections.

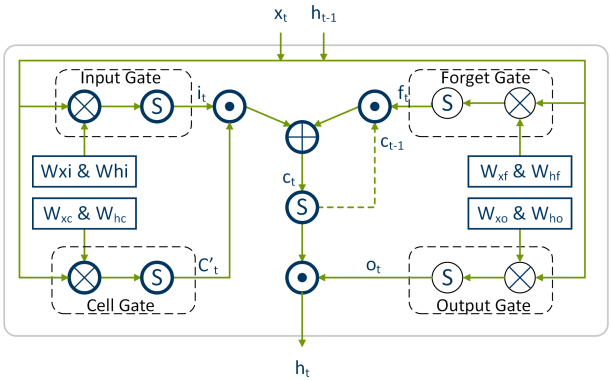

Figure 3. LSTM architecture with four gated units. The S denotes the Sigmoid function [7].

parallelism and batch processing. However, also ASIC and FPGA implementations can be beneficial. The acceleration of the feed-forward or inference path of DNNs on FPGAs offers benefits like a better utilization of fine-grained or heterogenous parallelism, as well as a higher energy-efficiency and flexibility. These advantages are especially interesting with respect to the application of DNNs on embedded devices. In this paper, we focus on analyzing different hardware architectures, mainly FPGA implementations, for accelerating CNNs and RNNs. The structure of our paper is as follows: Section I briefly introduces our paper with a description of CNNs, RNNs and their implementation platforms. Section II presents an overview of the recent implementations of CNNs. Next, Section III describes an analysis on the implementation of CNNs on FPGAs boards. Similarly, Section IV presents an analysis of recent implementations of RNNs on FPGA boards. Finally, Section V presents the concluding remarks of our work.

II. Overview of Convolutional Neural Networks Implementations

Within this section, we give an overview about multiple CNN implementations. The following Section III discusses FPGA implementations in more detail.

A. ASIC-based Implementations

ASIC-based approaches offer great performance and low power capabilities; however, they lack flexibility and have a larger design flow process. The approaches based on this platform are highly customized for an application. Under this category, Chen et al. [11] introduced $Eyeriss$, accelerator for deep CNNs that aims for energy efficiency. The accelerator consists of a Static Random-Access Memory (SRAM) buffer that stores input image data, filter weights and partial sums to allow fast reuse of loaded data. This data is streamed to a spatial array of 14x12 Processing Engines (PE), which compute inner products between the image and filter weights. Each PE consists of a pipeline of three stages that computes the inner product of the input image and filter weights of a single row of the filter. The PE also contains local scratch pads that allow temporal reuse of the input image and filter weights to save energy. There is also another scratch pad in charge of storing partial sums generated for different images, channels or filters, also with the aim of reusing data and saving energy. To optimize data movement, the authors also propose a set of input Network on Chips (NoC), for filter, image and partial sum values, where a single buffer read is used by multiple PEs. This approach was implemented in a $65nm$ CMOS, achieving a frame rate $44.8fps$ and a core frequency of $250MHz$.

Korekado et al. [12] propose an analog-digital hybrid architecture for CNNs for image recognition applications, focusing on high performance at low power consumption. The architecture consists of a pulse-width modulation circuit to compute the most common operations of a CNN and a digital memory to store intermediate results, making use of a time-sharing technique to execute the operations required by all

the connections of the network with the restricted number of processing circuits available in the chip. This architecture was implemented in a $0.35\mu m$ CMOS. The paper reports an execution time of $5ms$ for a network with 81 neurons and 1620 synapses, an operation performance of 2 Giga Operations Per Second (GOPS) and a power consumption of $20mW$ for the Pules Width Modulation (PWM) neuron circuits and $190mW$ for the digital circuit block.

Andri et al. [13] present $Yodann$, an ASIC architecture for ultra-low power binary-weight CNN acceleration. In this work, a binary-weight CNN is chosen for implementation because limiting a CNN's weights to only two values (+1/-1) avoids the need of expensive operations such as multiplications, which can be replaced by simpler complement operations and multiplexers, thus reducing weight storage requirements. This also has the advantage of reducing I/O operations. Moreover, this approach implements also a latch-based standard cell memory (SCM) architecture with clock-gating, which provide better voltage scalability and energy efficiency than SRAMs, at the cost of a higher area consumption. The architecture was implemented using UMC $65nm$ standard cells using a voltage range of $0.6V - 1.2V$. The article reports a maximum frequency of $480MHz$ at $1.2V$ and $27.5MHz$ at $0.6V$ and an area of 1.3 Million Gate Equivalent (MGE).

B. GPU-based Implementations

Recently, GPUs have been used as an implementation platform for highly parallelizable algorithms. While they offer more flexibility than the ASICs, they are more limited than the FPGAs in terms of customization capabilities. Ciresan et al. [14] presents a parameterizable GPU implementation for CNN variants. This implementation enables the user to configure several structural CNN parameters such as: input image size, number of hidden layers, number of maps per layer, kernel sizes, skipping factors and connection tables. Regarding the architecture, this implementation consists of three main CUDA kernels: Forward Propagation (FP), Backward Propagation (BP) and Adjusting Weights (AW). In the FP and BP kernels, each map of a CNN that has to be computed is assigned a different thread block to allow parallelization. The AW kernel is implemented as a 1D grid, with one block located between each connection between two maps, where each block is a 2D grid, with a corresponding thread for every kernel weight. This approach was evaluated with a set of benchmarks for different applications in the domain of object recognition: digit recognition (MNIST), 3D object recognition (NORB [15]) and natural images (CIFAR10 [16]). The authors report a speedup of 10 to 60 in comparison with a compiler optimized CPU. Moreover, this approach has been used to implement deep neural networks for traffic sign classification, which achieved a better-than-human recognition rate [17] and for automatic segmentation of neuronal structures from stacks of Electron Microscopy (EM) images [18]. Furthermore, in order to ease the implementation of deep learning approaches on GPUs, some frameworks and libraries have been proposed as well.

C. FPGA-based Implementations

FPGA-based approaches take advantage of the flexibility and rapid-prototyping capabilities that this platform offers. However, FPGAs are still more power hungry than ASICs. A highly cited deep learning approach implemented on an FPGA is the one of Farabet et al. [19], a hardware architecture to accelerate CNNs for synthetic vision systems. The architecture consists of a control unit, several parallel ALUs/Streaming operators and a memory interface streaming engine. The ALUs implement operators required by bio-inspired CNNs, such as 2D convolver, dot products between a vector and multiple 2D planes, spatial pooling, arbitrary non-linear mappings, element-wise multiplication of a vector by another one. This approach was implemented in a CPU, an FPGA (a Xilinx Virtex-4 SX35) and was also simulated for an ASIC.

Chakradhar et al. [20] propose a co-processor configurable architecture to accelerate CNNs. The authors show evidence of how different workloads and different number of inputs and outputs need different network architectures to yield optimal performance. Thus, they propose an architecture that analyses workloads, can configure the number of convolvers in a computational element and also, the number of computational elements in the whole network to match the types of parallelism of every workload. The architecture was implemented on a Virtex 5 SX240T FPGA and was compared against the best fixed architecture for a set of benchmark applications.

Farabet et al. [21] introduce $NeuFlow$, which is a reconfigurable dataflow processor for vision algorithms. The architecture of this processor consists of a 2D grid of $ProcessingTiles$ (PT). Each PT can be configured to carry out operations on a stream of data, from unary operations to complex nested operations. The grid is connected to a $SmartDMA$, which is connected to an Off-chip memory. The $SmartDMA$ allows the control unit to configure the grid and the DMA ports for each operation and to carry the data from the grid to the off-chip memory in parallel. To configure the processor for a particular algorithm, a compiler called $LuaFlow$ was developed. This compiler takes a tree or a graph structure that represents the algorithm and parses it to determine the parallelism of the algorithm that the processor can take advantage of. This approach was implemented on a Xilinx Virtex 6 ML605 FPGA board at $200MHz$ using 10x10 grids. At its peak performance, the design achieved 80 billion connections per second. Furthermore, a CNN for street scene parsing was implemented on this platform, achieving a performance of $12fps$.

It is hard, if not impossible, to generate a fair comparison among all the described approaches, because they were either designed for different applications with different constraints and objectives or they were implemented using different devices with different configurations. Table I shows a summary of these values, categorized by the three main implementation platforms. Furthermore, the following section will stablish a comparison between approaches from the year 2016 against that of 2011.

III. Analysis of CNN Implementation FPGAs

The selected baseline FPGU implementation of Farabet et al. is presented in [21] and [24]. The modules are implemented on the processing tiles according to the operators contained in each of them, for instance, those with multiply-accumulate operators can be used to execute a 2D convolution (*Convolutional module*) while those with the *tanh operator* are dedicated to the non-linear module.

For the pooling layer, it is possible to use the same processing tiles mentioned before for the convolution module.

TABLE I. COMPARISON OF CNN IMPLEMENTATION APPROACHES

Platform	Approach	Device	Core Frequency	Power	FPS	Performance	Area
ASIC	Eyeriss [11]	65nm CMOS	100 - 250MHz	278 mW at 1V	44.8	16.8 - 42 GOPS	1852 kGates
	[12]	0.36μm CMOS		20mW PWM circuit + 190 mW digital core		2 GOPS	
	Yodann [13]	65nm UMC	27.5MHz-480MHz	895μW	11 - 16.8	1.5 TOPS	1.3 MGE
	[19]	ASIC Simulation	400MHz	1W	>30		
FPGA	[19]	Xilinx Virtex-4 SX35	200MHz	15W	> 30		
	[20]	Virtex 5 SX240T	120MHz	<14W	25 - 30		
	NeuFlow[21]	Virtex 6 ML605	200MHz	10W	12	160 GOPS	
	[22]	Altera Stratix	130MHz		1600	409.622 GOPS	
	[23]	Xilinx Kintex-7		<4W		247 GOPS	
GPU	[14]	1 CPU: Core i7-920, 4 GPU: 2 x GTX 480, 2 x GTX 580	2.66 GHz (CPU)			10-60 speedup vs CPU	

Here is also stated that it is advantageous to use a 16Bit format instead of a 32, then, even though a loss of precision is caused, this is not a relevant loss. The results on each of the processing tiles is also pipelined to obtain a result for each clock cycle.

This approach was tested on the datasets NORB[**?**], MNISt[25] and UMASS[26] obtaining correct classification between 85% and 98% depending on the dataset.

The next step is to present 2 papers published 5 years later, in 2016, claiming to have encountered a novel and performant implementation.

On the one hand, Li et al. [22] focus on High-speed image classification, mentioning that the implementation presented can be useful if implemented in a rear-end collision avoidance system. On the other hand, Dundar et al. [23] warrant that the approach supports different configurations of deep CNNs, disregarding layers depth, filter quantity or others, and it is stated that the a perfect scenario for its application is the generic image processing. The former utilizes an Altera Stratix V 5SGSMD5K2F40C2 FPGA while the latter a Xilinx Kintex-7 XC7K325T.

On the filter layer, [22] utilizes 3D convolvers for each filter. These are composed of multiple 2D convolvers that calculate one channel of the filter. The 2D convolvers contain the so called *Processing Elements (PE)* connected under a First-In First-Out (FIFO) queue. The PE are, at their time, composed f multipliers and adders, like the processing tiles presented before, plus a register of one word length.

For [23] the convolution on this layer is done with trained filters to obtain remarking features from the images. The weights are represented as 4D filters.

For the non-linear module, both researches employ Rectified-Linear Units (ReLU) since it is said to be more suitable to implement in Hardware.

There are, again, some differences in the pooling layer, where [22] considers an approach closer to the one presented in [24] where the pooling and filter bank layer are executed in a similar fashion, even if with some minor modifications. These differences are, for example, that the PEs compare two different values and return only the higher value, reducing the output and energy consumption, this is not present in [19]. For [23] however, the approach is similar. The input images of the layer are divided in smaller squares, windows, and in a comparable manner to the previously explained, only the maximum value of the resulting set is to be outputted, this is a mode of non-linear down-sampling, and the factor of down-sampling is equal to the size of the windows.

As a novel idea for improving the performance of the system, [22] presents the *Global Summation*, designed to minimize resource consumption on the latest layers in favor of the overall performance. In contrast, [23] presents several techniques to improve the control method of the process, among several improvements. For instance, it is important to mention the *input reuse* and the *concatenation of data*. The Input reuse, consists of extending the information to convolution modules even though if the amount of available ports is smaller than that of free convolution modules. Those convolution modules that have access to the port can share the information to those who are idle. The concatenation of data profits of the Q8.8 format. The Q8.8 format uses 16 bits in a 32 stream, so that 2 different data words can be transmitted in a unique stream

Finally, these implementations were tested on datasets, in the case of [22], this was done over two different datasets, the first consisting of several images from the datasets CIFAR[16], CBCL[27] and Caltech Cars [28]. The second one consisted of edited images from Caltech Cars and CBCL car dataset. They achieved 94.5% in the first case and 98.4% in the second. The system is said to be performant at 1,600 frames per second and according to estimations of the authors, they obtain 409,62 GOPS.

[23] on the contrary, was tested on an own dataset utilizing videos and sets of images from these videos. Their work was compared to a GPU NVIDIA K40, a Zynq ARM Cortex A9 at 667MHz, an Intel Core i7 at 2.5GHz and a naïve implementation of a hardware accelerator. Regarding performance per second, the GPU turned to be victorious with a huge advantage over the others, however, when calculating the performance per Watt, the implementation presented was more performant than the others. The authors mentioned to have a peak in the performance at 247 GOPS.

Both approaches present FPGAs as a tool for accelerating deep CNNs and both belong to the newest researches on this field. The improvement on the performance of each implementation is notable when compared to an implementation 5 years older. However, the core idea of the accelerator presented in 2011 is still present in these two newer papers.

When comparing the three CNN modules, the approaches shared similarities, as for example, the use of ReLU for the activation layer, instead a sigmoid function or a tanh operation.

Copyright (c) IARIA, 2017. ISBN: 978-1-61208-549-4

Another important similarity is to be found in the pooling layer, where only the higher value of the resulting set is to be outputted.

The difference between these approaches lies in the implementation of the convolutional layer, where the representation of the filters is very different for each of them.

Another small but very important similarity is the usage of the number format Q8.8, of 16 bits. [23] goes further and takes advantage of this by sending two different words in a single bitstream. Important is also to notice that [22] used well known datasets, CIFAR, Caltech cars, to test this approach, while [23] used their own dataset. When comparing the value of GOPS, [22] has a value that almost doubles the highest peak of [23]. However this value is obtained from a simulation of the model while the value on [23] is an output design.

IV. Analysis of RNN Implementations on FPGAs

In general, two possibilities exist to increase the overall performance of RNNs regarding the inference phase on FPGAs. On one hand the computations which must be done while passing the input through the network can be optimized. This includes adjusting the level of parallelism due to the hardware constraints, the choice of hardware accelerator module and approximations of computation, in case of an acceptable minimal loss of precision. On the other hand, the data communication, which includes weight parameters and inputs, between the FPGA and an external memory, like Dynamic Random Access Memory (DRAM), can be optimized to improve the throughput. This is necessary because typically the FPGA on-chip-memory, like Block RAM (BRAM) or distributed memory, is too small to store all parameters of real-life RNNs. Thus, the developer of FPGA accelerators for RNNs have to consider both optimization paths. Moreover, to increase the overall performance both optimizations paths must collaborate to avoid bottlenecks.

Guan et al. [7] faced both optimization paths. After profiling a typical RNN inference structure they found out that the main bottleneck is caused by the computations, which mainly include floating point multiplication and addition, inside each LSTM gate. Therefore, they separate the computation scheme (Fig.3) into four LSTM gate modules, which output the input, forget, cell and output gate vector executed in parallel, and a LSTM Functional Logic, which includes the following computations. Inside each gate the multiplications of input and parameter vector are also done in parallel and summed up through an addition tree. The activation function at the end of each gate module and the LSTM functional logic are replaced with a piecewise linear approximation of $sigmoid$ and $tanh$, which was originally introduced by Amin et al. [29]. As a result, resource and performance inefficient computations are substituted with simpler and more hardware efficient addition and shifting operations with a minimal loss of accuracy. Furthermore, two input and output ping-pong buffer groups are improving the communication performance. The parameters are stored in an external DRAM and reshaped offline so that the data access can be done in a sequential manner. Moreover, a data dispatcher is used to interface the DRAM with full burst size of the AXI4 bus. The Accelerator is designed with a High-Level Synthesis tool (HLS), Vivado HLS from Xilinx [30] and the system is implemented on a XILINX VC707 device with a Virtex7 FPGA chip. The evaluation shows that the system achieves a maximum performance of 7.26 GFLOP/S.

A different architecture is proposed by Chang et al. [31]. Like in the previous architecture, they use two different hardware accelerator modules, to separate gating and LSTM-logic computations. Another similarity is the simplification of the nonlinear activation function through piecewise linear approximation. In contrast to the previous design Chang et al. [31] use fixed point 16-bit operations for MAC (Multiply Accumulate) operations resulting in 32 bit values for further operations. While fixed-point computations are far more efficient for hardware implementations, a loss of accuracy has to be considered what was denoted as a maximum of 7.1. Furthermore, the gating computations are separated into two sequential steps. The input and cell gate computations are done in parallel as well as the output and forget gate computations. As a result, the output of the LSTM module is provided after 3 sequential steps. Thus, the course grained parallelism is not fully exploded. For communication optimization, the authors of [31] use a combination of memory mapping and streaming interface. Therefore, four Direct Memory Access (DMA) are used to access the external DRAM and reshape the data to be forwarded through 8 AXI4-Stream, which activity depends on the current routing, and buffered with FIFOs. In comparison to the communication architecture presented by Guan et al. [7] the methodology is equal but the differences in implementation details mainly arise because of the different course grained parallelism of the LSTM accelerator. The design is implemented on a Zedboard with Zynq 7020 FPGA from Xilinx. The hardware was tested with a two-layer LSTM including 128 hidden units running with a frequency of 142MHz. The performance was outlined to 264.4 million operations per second.

In contrast to [31] and [7] the authors of [32] use a retrained based method to reduce the word-length of the weights. As a result, they achieve a quantification to 6 bits per weight. Due to this fact, for the desired speech recognition application all weight parameters can be stored on the on-chip-memory (BRAM) on the XC7Z045 FGPA device from Xilinx without loss of precision differences of retraining and hardware implemented inference computation. Without the requirement to optimize the communication from an external DRAM the focus of this work is the accelerator module optimization. Although the proposed LSTM accelerator module is separated into two different modules the parallelism and task granularity differ from those proposed in [7] and [31]. All matrix-vector multiplications are computed inside one Processing Element (PE) array, which consist of 512 PEs. The remaining computations including evaluating activation functions are done using an additional block called Extra Processing Unit (EPU). The outputs of the PE array are buffered and forwarded to the LSTM EPU. As mentioned above, the design benefits from a high level of fine-grained parallelism. However, the architecture is not comparable to the other design as no communication bottleneck has to be handled and the authors focus on the optimization of the whole speech recognition algorithm while considering real-time constraints for the desired application.

Besides, Ferreira et al. [33] follow a modular extensible architecture. They assume a similar reduction of communication complexity as assumed in [32]. In contrast to [32] the word-length of the weights are 18 bits, which leads

to a high utilization of the Digital Signal Processor (DSP) DSP48E1 slices of the FPGA, and they are stored in a Look-up RAM (LUTRAM). On the one hand, this distributed memory represents the fastest way of accessing the weights due to the closeness to the accelerator and the unlimited simultaneous port access to each LUTRAM array. In contrast, BRAM supports a maximum of two port access. On the other hand, this method consumes a high amount of resources especially when the implemented network has many layers and LSTM-tiles. The architecture does not explore full parallelism in a coarse-grained manner. The matrix-vector multiplications are done in parallel for all four gates. Due to the negligible amount of additional clock cycles needed for elementwise multiplication and activation function evaluation of $tanh()$ and $sigmoid()$, which are approximated with ridge (polynomial) regression. Each of these computations own one hardware module. The gate outputs are forwarded to a multiplexer and further routed to the desired hardware module. The design was implemented on a Xilinx XC 7Z020SoC device with different amounts of neurons per layer. The network size is not allowed to extend 31 neurons per layer due to the limited number of DSP-slices on the device. The frequency of the hardware accelerator was adjusted to maximum with respect to the layer size. Thus, the design is capable of achieving 4534.8 million operation per second, which is 17 times more than the performance reached in [31].

V. Conclusion

As outlined in the previous sections, there are many possibilities to accelerate CNNs or RNNs with the help of hardware modules. Each of these hardware implementations has a significant speedup in comparison to a CPU implementation. From our perspective, there are several reasons making a fair comparison of all hardware architectures not possible. One of that reasons is that the size of the networks mostly depends on the application as well as the real-time constraints. Thus, a good hardware implementation reduces energy and resource consumption without validating real-time constraints.

Regarding the evolution of the implementation of CNNs on a FPGA over five years, it is remarkable that the core framework has not changed abruptly in this time lapse, where the researches utilizes different FPGUs platforms. Nevertheless, the most important object of study are the modules. These different approaches apply different metrics to stablish the performance success, i.e. some use GOPS, FLOPS or Fps, while other focus on the energy consumed, making a direct comparison among them a very hard task. It would be ideal if a baseline reference statistics could be defined, so that future works compare themselves to this baseline. As Table I shows, even though the performance between FPGA and ASIC approaches are comparable, the reported power consumption values of the latter are lower. This is usually the tradeoff between FPGA and ASIC implementations, i.e. higher flexibility but higher power consumption. However, this can be improved by simplifying the DNN architecture with little loss of accuracy. One nice example of this are BNNs [13], which achieve a competitive accuracy and greatly decease power consumption. This simplification could be also coupled with the reconfiguration capabilities of FPGAs, such that this tradeoff of accuracy and power consumption can be adapted to the requirements of the application [20].

References

[1] I. Goodfellow, Y. Bengio, and A. Courville, Deep Learning. MIT Press, 2016, http://www.deeplearningbook.org.

[2] W. Zhao, S. Du, and W. J. Emery, "Object-based convolutional neural network for high-resolution imagery classification," IEEE Journal of Selected Topics in Applied Earth Observations and Remote Sensing, vol. PP, no. 99, 2017, pp. 1–11.

[3] H. J. Jeong, M. J. Lee, and Y. G. Ha, "Integrated learning system for object recognition from images based on convolutional neural network," in 2016 International Conference on Computational Science and Computational Intelligence (CSCI), Dec 2016, pp. 824–828.

[4] T. He and J. Droppo, "Exploiting lstm structure in deep neural networks for speech recognition," in 2016 IEEE International Conference on Acoustics, Speech and Signal Processing (ICASSP), March 2016, pp. 5445–5449.

[5] A. Krizhevsky, I. Sutskever, and G. E. Hinton, "Imagenet classification with deep convolutional neural networks," in Advances in Neural Information Processing Systems 25, F. Pereira, C. J. C. Burges, L. Bottou, and K. Q. Weinberger, Eds. Curran Associates, Inc., 2012, pp. 1097–1105, last accessed March 27th, 2017. [Online]. Available: http://papers.nips.cc/paper/4824-imagenet-classification-with-deep-convolutional-neural-networks.pdf

[6] J. Chung, Ç. Gülçehre, K. Cho, and Y. Bengio, "Empirical evaluation of gated recurrent neural networks on sequence modeling," CoRR, vol. abs/1412.3555, 2014, last accessed March 28th, 2017. [Online]. Available: http://arxiv.org/abs/1412.3555

[7] Y. Guan, Z. Yuan, G. Sun, and J. Cong, "Fpga-based accelerator for long short-term memory recurrent neural networks," in 2017 22nd Asia and South Pacific Design Automation Conference (ASP-DAC), Jan 2017, pp. 629–634.

[8] L. C. Jain and L. R. Medsker, Recurrent Neural Networks: Design and Applications. CRC Press, Inc., 2001.

[9] S. Hochreiter and J. Schmidhuber, "Long short-term memory," Neural Computation, vol. 9, no. 8, Nov 1997, pp. 1735–1780.

[10] D. Strigl, K. Kofler, and S. Podlipnig, "Performance and scalability of gpu-based convolutional neural networks," in Parallel, Distributed and Network-Based Processing (PDP), 2010 18th Euromicro International Conference on. IEEE, 2010, pp. 317–324.

[11] Y.-H. Chen, T. Krishna, J. S. Emer, and V. Sze, "Eyeriss: An energy-efficient reconfigurable accelerator for deep convolutional neural networks," IEEE Journal of Solid-State Circuits, vol. 52, no. 1, 2017, pp. 127–138.

[12] K. Korekado, T. Morie, O. Nomura, H. Ando, T. Nakano, M. Matsugu, and A. Iwata, "A convolutional neural network vlsi for image recognition using merged/mixed analog-digital architecture," in Knowledge-Based Intelligent Information and Engineering Systems. Springer, 2003, pp. 169–176.

[13] R. Andri, L. Cavigelli, D. Rossi, and L. Benini, "Yodann: An architecture for ultra-low power binary-weight cnn acceleration," IEEE Transactions on Computer-Aided Design of Integrated Circuits and Systems, vol. PP, no. 99, 2017, pp. 1–1.

[14] D. C. Ciresan, U. Meier, J. Masci, L. Maria Gambardella, and J. Schmidhuber, "Flexible, high performance convolutional neural networks for image classification," in IJCAI Proceedings-International Joint Conference on Artificial Intelligence, vol. 22, no. 1. Barcelona, Spain, 2011, p. 1237.

[15] "NORB Dataset," http://www.cs.nyu.edu/ ylclab/data/norb-v1.0/, accessed: 2017-04-15.

[16] "CIFAR Dataset," https://www.cs.toronto.edu/ kriz/cifar.html, accessed: 2017-04-15.

[17] D. CireşAn, U. Meier, J. Masci, and J. Schmidhuber, "Multi-column deep neural network for traffic sign classification," Neural Networks, vol. 32, 2012, pp. 333–338.

[18] D. Ciresan, A. Giusti, L. M. Gambardella, and J. Schmidhuber, "Deep neural networks segment neuronal membranes in electron microscopy images," in Advances in neural information processing systems, 2012, pp. 2843–2851.

[19] C. Farabet, B. Martini, P. Akselrod, S. Talay, Y. LeCun, and E. Culurciello, "Hardware accelerated convolutional neural networks for syn-

thetic vision systems," in Circuits and Systems (ISCAS), Proceedings of 2010 IEEE International Symposium on. IEEE, 2010, pp. 257–260.

[20] S. Chakradhar, M. Sankaradas, V. Jakkula, and S. Cadambi, "A dynamically configurable coprocessor for convolutional neural networks," in ACM SIGARCH Computer Architecture News, vol. 38, no. 3. ACM, 2010, pp. 247–257.

[21] C. Farabet, B. Martini, B. Corda, P. Akselrod, E. Culurciello, and Y. LeCun, "Neuflow: A runtime reconfigurable dataflow processor for vision," in Computer Vision and Pattern Recognition Workshops (CVPRW), 2011 IEEE Computer Society Conference on. IEEE, 2011, pp. 109–116.

[22] N. Li, S. Takaki, Y. Tomiokay, and H. Kitazawa, "A multistage dataflow implementation of a deep convolutional neural network based on fpga for high-speed object recognition," in 2016 IEEE Southwest Symposium on Image Analysis and Interpretation (SSIAI), March 2016, pp. 165–168.

[23] A. Dundar, J. Jin, B. Martini, and E. Culurciello, "Embedded streaming deep neural networks accelerator with applications," IEEE Transactions on Neural Networks and Learning Systems, vol. PP, no. 99, 2016, pp. 1–12.

[24] C. Farabet, Y. LeCun, K. Kavukcuoglu, and E. Culurciello, "Large-scale fpga-based convolutional networks," Scaling up Machine Learning: Parallel and Distributed Approaches, pp. 399–419.

[25] "MNIST Dataset," http://yann.lecun.com/exdb/mnist/, accessed: 2017-04-15.

[26] "UMAss Dataset," https://www.umass.edu/statdata/statdata/index.html, accessed: 2017-04-15.

[27] "CBCL Dataset," http://poggio-lab.mit.edu/, accessed: 2017-04-15.

[28] "CALTECH Dataset," http://www.vision.caltech.edu/archive.html, accessed: 2017-04-15.

[29] H. Amin, K. M. Curtis, and B. R. Hayes-Gill, "Piecewise linear approximation applied to nonlinear function of a neural network," IEE Proceedings - Circuits, Devices and Systems, vol. 144, no. 6, Dec 1997, pp. 313–317.

[30] "Vivado hls," https://www.xilinx.com/products/design-tools/vivado/integration/esl-design.html, accessed: 2017-04-15.

[31] E. C. Andre Xian Ming Chang, Berin Martini, "Recurrent neural networks hardware implementation on fpga," in arXiv preprint arXiv:1511.05552, 2015.

[32] M. Lee, K. Hwang, J. Park, S. Choi, S. Shin, and W. Sung, "Fpga-based low-power speech recognition with recurrent neural networks," in 2016 IEEE International Workshop on Signal Processing Systems (SiPS), Oct 2016, pp. 230–235.

[33] J. C. Ferreira and J. Fonseca, "An fpga implementation of a long short-term memory neural network," in 2016 International Conference on ReConFigurable Computing and FPGAs (ReConFig), Nov 2016, pp. 1–8.